

AD-A125 182

EFFECT OF AN INHOMOGENEOUS TRANSITION LAYER ON THE
RESPONSE OF A COMPLIAN. (U) SAN DIEGO STATE UNIV CA
DEPT OF AEROSPACE ENGINEERING AND ENG.
M PIERUCCI ET AL. JAN 83

1/1

UNCLASSIFIED

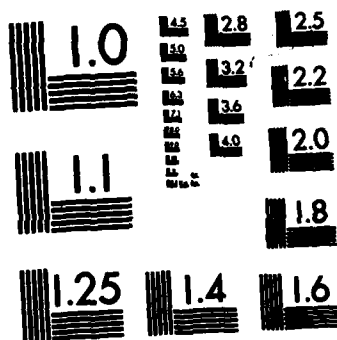
F/G 20/4.

NL

END

FILED

DTIC



MICROCOPY RESOLUTION TEST CHART
NATIONAL BUREAU OF STANDARDS-1963-A

SDSU - AE&EM TR 83-01

Effect of an Inhomogeneous Transition Layer on the Response of a Compliant Layer Due to a Shear Fluid Disturbance

Mauro Pierucci
Paul A. Baxley

January 1983

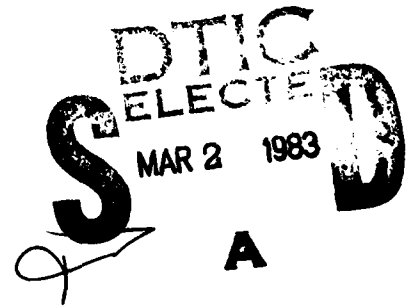
*Research Sponsored by Office of Naval Research
under Contract N00014-81-K-0424*

Approved for Public Release - Distribution Unlimited

DTIC FILE COPY

AD A125162

SAN DIEGO STATE UNIVERSITY
College of Engineering
Department of Aerospace Engineering
and Engineering Mechanics
San Diego, CA 92182
(619) 265-6074



83 03 02 037

ABSTRACT

The amount of interaction between a fluid and a compliant coating is studied for a one dimensional shear fluid disturbance. A thin inhomogeneous viscoelastic layer is located at the interface between the fluid and the coating. The fluid is assumed to have no mean flow field. The effect of different coating properties, thickness of compliant coating and of transition layer as well as the frequency of oscillations are analyzed.



Accession For	
NTIS GRA&I	<input checked="checked" type="checkbox"/>
DTIC TAB	<input type="checkbox"/>
Unannounced	<input type="checkbox"/>
Justification	
By	
Distribution/	
Availability Codes	
Dist	Avail and/or Special
A	

TABLE OF CONTENTS

I. INTRODUCTION

II. ANALYSIS

- 1. Fluid**
- 2. Solid**
- 3. Unified Theory**
- 4. Solution**

III. DISCUSSION OF RESULTS

IV. CONCLUSIONS

V. REFERENCES

FIGURES

APPENDIX

I. INTRODUCTION

The drag of a body can be decreased by a compliant coating only if a considerable amount of interaction exists between the fluid and the coating. The coating has to be able to be excited by a fluid disturbance and, in turn, the coating disturbance has to change the characteristics of the fluid disturbance in such manner as to decrease the overall drag of the body.

In typical applications, the flow field will have either a laminar or a turbulent boundary layer. For low Reynolds numbers (air application), the boundary layer will typically be laminar whereas for high Reynolds numbers (underwater application) the boundary layer will be turbulent. The interaction phenomenon required for drag reduction may be totally different in the two cases. The drag of a body with a laminar boundary layer will consist mostly of the drag due to skin friction. The drag of the same body but with a turbulent boundary layer will, however, be influenced the most by the magnitude of the Reynolds turbulent stresses. The drag due to the laminar sublayer is always smaller than the drag due to the normal Reynolds stresses acting on a wavy wall (fig. 1).

In order to properly model the fluid-structure interaction, as represented by the flow fields discussed above, two types of fluid disturbance should be analyzed: shear disturbance and normal (or longitudinal) disturbance. The shear disturbance will serve to simulate the interaction of the fluid

with the coating for either the laminar boundary layer case or the laminar sublayer underneath the turbulent boundary layer. The longitudinal (or acoustic) disturbance result will be used to model the interaction between the Reynolds turbulent stresses and the compliant surface.

The parameters which govern the local properties of a one dimensional medium can be taken to be the density and the local wave speed of the medium. A disturbance traveling in a given direction will be partially reflected whenever a discontinuity in the properties of the medium exist. The interface between a coating and a fluid is an example of a medium discontinuity. If the effect of the discontinuity could be ameliorated then the reflection and the transmission of energy from one medium to another could be changed. A transition layer which spreads out the discontinuity between the two media, in a gradual manner, can be expected to increase the magnitude of the interaction between the two media. The properties of the transition layer may vary continuously from that of a solid on one side to that of a fluid on the other side. Alternatively, the transition layer may be assumed to be an equivalent layer whose properties are determined by the overall local motion of the surface of the coating (Fig.(2)). The transition layer will thus exhibit the properties of an inhomogeneous layer with continuously varying properties (Fig. (3)). Thus the transition layer can either be designed as part of the compliant coating or it can be thought to be an integral part of the coating with the mean transition layer properties due mainly to the

inability to properly identify the location of the interface being forced in a random manner by the turbulence; in this context, then the transition layer will acquire average properties of the solid and the fluid and the actual magnitude of the properties will depend upon the average of the space-time history of the surface motion at each location.

In the two previous reports,^{1,2} the distribution of both shear and normal disturbances, due to a disturbance at the bottom of the compliant coating were studied (Fig. (4)). The results indicated that the transmission of shear disturbances into the fluid can be altered considerably by the presence of a thin transition layer.¹ For the same conditions, longitudinal (or normal) wall disturbances will be affected by the transition layer in a much reduced manner.

Pedersen et al³ have shown that an inhomogeneous layer with an exponentially varying impedance at the interface varying from that of a solid to that of a fluid increases the acoustic energy transmitted from the solid into the fluid.

II. ANALYSIS

The analysis consists of the derivation of the governing equations for the fluid, the elastic solid and the transition layer and the numerical technique utilized to integrate the resulting differential equations.

II.1 Fluid

Consider a one dimensional fluid disturbance located at a distance h from the lower wall (Fig (3)). The equations governing the fluid motion, in its most general form are the Navier-Stokes equations and the continuity equation.

$$\rho \frac{Dv_1}{Dt} = \frac{\partial \tau_{11f}}{\partial x} + \frac{\partial \tau_{12f}}{\partial y} , \quad (1)$$

$$\rho \frac{Dv_2}{Dt} = \frac{\partial \tau_{21f}}{\partial x} + \frac{\partial \tau_{22f}}{\partial y} , \quad (2)$$

$$\frac{D\rho}{Dt} + \rho \left(\frac{\partial v_1}{\partial x} + \frac{\partial v_2}{\partial y} \right) = 0 , \quad (3)$$

where $\frac{D}{Dt}$ is the material derivative and is given by

$$\frac{D}{Dt} = \frac{\partial}{\partial t} + v_1 \frac{\partial}{\partial x} + v_2 \frac{\partial}{\partial y} . \quad (4)$$

v_1 and v_2 are the local fluid velocities in the x and the y

direction respectively and ρ_f is the fluid density. The fluid stresses τ_{11f} , τ_{12f} , τ_{21f} and τ_{22f} are given by

$$\tau_{11f} = -p + \mu \left[\frac{4}{3} \frac{\partial v_1}{\partial x} - \frac{2}{3} \frac{\partial v_2}{\partial y} \right] , \quad (5)$$

$$\tau_{12f} = \tau_{21f} = \mu \left[\frac{\partial v_1}{\partial y} + \frac{\partial v_2}{\partial x} \right] , \quad (6)$$

$$\tau_{22f} = -p + \mu \left[-\frac{2}{3} \frac{\partial v_1}{\partial x} + \frac{4}{3} \frac{\partial v_2}{\partial y} \right] . \quad (7)$$

where μ is the fluid viscosity.

For a one dimensional fluid shear disturbance, the v_2 component of velocity term will be zero. If the fluid disturbance is assumed to vary sinusoidally in time,

$$v_1 = v_1 \exp(-i\omega t) , \quad (8)$$

then the governing equation reduces to

$$\frac{d}{dy} \left(\mu \frac{dv_1}{dy} \right) + i\rho_f \omega v_1 = 0 . \quad (9)$$

II.2 Solid

The fluid disturbance will propagate from its source to the fluid-solid interface, where the no slip condition and the

continuity of stress will cause the disturbance to propagate into the fluid.

The generalized equations for the motion of the solid are the Navier equations:

$$\rho_s \frac{\partial^2 u_1}{\partial t^2} = \frac{\partial \tau_{11s}}{\partial x} + \frac{\partial \tau_{12s}}{\partial y}, \quad (10)$$

$$\rho_s \frac{\partial^2 u_2}{\partial t^2} = \frac{\partial \tau_{21s}}{\partial x} + \frac{\partial \tau_{22s}}{\partial y}, \quad (11)$$

where ρ_s is the density of the material. The solid particle displacements in the x and the y direction are u_1 and u_2 respectively. The solid stresses are linearly related to the particle displacements u_1 and u_2 ,

$$\tau_{11s} = \frac{2G}{1-2\nu} \left[(1-\nu) \frac{\partial u_1}{\partial x} + \nu \frac{\partial u_2}{\partial y} \right], \quad (12)$$

$$\tau_{12s} = \tau_{21s} = G \left[\frac{\partial u_1}{\partial y} + \frac{\partial u_2}{\partial x} \right], \quad (13)$$

$$\tau_{22s} = \frac{2G}{1-2\nu} \left[\nu \frac{\partial u_1}{\partial x} + (1-\nu) \frac{\partial u_2}{\partial y} \right], \quad (14)$$

where G is the shear modulus and ν is Poisson ratio. In general G will be a real number if the solid is purely elastic and a complex number if the material has damping properties.

If the fluid disturbance is a shear vibration and is independent of its x location then the solid will, by necessity, vibrate in a similar fashion; thus equations 10-14 are combined into an ordinary differential equation

$$\frac{d}{dy} \left(G \frac{du_1}{dy} \right) - \rho_s \omega^2 u_1 = 0 \quad (15)$$

For an inhomogeneous viscoelastic medium, the shear modulus G will be a complex function of y .

II.3 Unified Theory

The differential equation governing the fluid motion (Eq. 9) and the equation governing the solid motion (Eq. 15) are seen to be very similar. For a fluid disturbance with no mean flow field, the fluid disturbance velocity v_1 is related to the particle displacement u_1 by

$$v_1 = -i\omega u_1 \quad (16)$$

The vibration of the fluid-solid system can be combined into a unified equation given by

$$\frac{d}{dy} \left(K \frac{du_1}{dy} \right) + \rho\omega^2 u_1 = 0 \quad (17)$$

The parameter K is given by

$$K = \frac{G \text{ solid}}{-i\omega\mu \text{ fluid}} \quad (18)$$

and the density ρ is either the solid or the fluid density. The transition layer interposed between the fluid and the solid will be assumed to vary exponentially from the shear modulus G on one side to the fluid viscosity μ on the other. The

discontinuous parameter K can thus be written as

$$K(y) = -i\mu\omega + [G + i\mu\omega] \exp(-y/\ell)^n \quad (19)$$

For values of y close to the inner wall, the elastic solid properties are recovered and for values of y far removed from the interface region (i.e. $y \gg \ell$), the fluid properties are obtained. In equation 19, ℓ is the nominal thickness of the compliant coating and n is inversely related to the thickness of the transition layer. In the limit as $n \rightarrow \infty$, the thickness of the transition layer approaches zero and the classical elastic-solid-viscous-fluid equations are recovered.

Equations (17) and (19) can be re-cast in dimensionless form and become

$$\frac{d}{dy} \left(H \frac{du_1}{dy} \right) + \Gamma^2 R u_1 = 0 \quad , \quad (17a)$$

$$H(y) = -iR + (1+iR) \exp(-y/\ell)^n \quad (19a)$$

H is defined to be equal to K non-dimensionalized with respect to the shear modulus G . For simplicity, it is assumed that the fluid and the solid have the same density; this is a good approximation for a rubber type of coating immersed in water. R is defined to be the square of the ratio of the speed of shear disturbances of the fluid to that of the elastic solid. Γ is defined as the ratio of nominal coating thickness ℓ to the fluid shear wavelength λ_f , thus

$$R = (c_f/c_s)^2 \quad , \quad (20)$$

$$\Gamma = 2\pi\ell/\lambda_f \quad . \quad (21)$$

The fluid shear wave speed c_f and the elastic solid transverse speed c_s are given by

$$c_f^2 = \mu\omega/\rho \quad , \quad (22)$$

$$c_s^2 = G/\rho \quad . \quad (23)$$

The parameters R and Γ can also be written as

$$R = \mu\omega/G = (\lambda_f/\lambda_s)^2 \quad , \quad (20a)$$

$$\Gamma = \omega\ell/c_f = \ell (\rho\omega/\mu)^{1/2} \quad . \quad (21a)$$

In the limiting conditions (i.e. $y \ll \ell$ and $y \gg \ell$), the unified system of equations reduce to the proper equations. For $y \ll \ell$, H equals to unity and equation 17a reduces to

$$\frac{d^2 u_1}{dy^2} + \Gamma^2 R u_1 = 0 \quad . \quad (24)$$

For $y \gg \ell$, H equals $-iR$ and the differential equation becomes

$$\frac{d^2 u_1}{dy^2} + i\Gamma^2 u_1 = 0 \quad . \quad (25)$$

II.4 Numerical Solutions

The governing unified differential equation

$$\frac{d}{dy} \left(H \frac{du_1}{dy} \right) + \Gamma^2 R u_1 = 0 \quad , \quad (17a)$$

is subject to the wall boundary condition and the imposed particle velocity at $y=h$; thus

$$u_1(0) = 0 \quad , \quad (26)$$

$$u_1(h) = 1 \quad . \quad (27)$$

Equation 17a subject the boundary conditions 26 and 27 is a split boundary value problem. The technique utilized to solve the differential equation is the Runge-Kutta numerical integration starting at $y=0$ and going out to $y=h$. The initial value of the slope of u_1 at $y=0$ is then iterated until the outer boundary condition $u_1(h)=1$ is satisfied. The iteration technique used is a linear interpolation and in most cases, 6-8 iterations are required to obtain accuracy of better than 0.1%. The step size required for the numerical integration is a function of the parameters R and Γ and varies from $y=0.01$ to $y=0.001$. In general, the smaller step size is required for either thicker coatings, thinner transition layers or higher frequencies.

It should be noted that all the parameters are complex numbers, so that the iteration on the initial slope of u_1 is really a double iteration, one on the real part of the derivative and the other on the imaginary part.

The complete copy of the computer program used to solve the system of equations can be found in the appendix.

III. DISCUSSION AND RESULTS

The results from the numerical integration of the equations is presented in the form of displacement, shear stress and power distribution from the disturbance location, through the transition layer and in the elastic coating.

The dimensionless parameters that have been studied are:

1. location of disturbance - h -,
2. thickness of transition layer - n -,
3. thickness of coating - ℓ -,
4. property of coating - R -.

The location of the disturbance is non-dimensionalized with respect to the nominal coating thickness ℓ . Thus values of h (fig. 1) less than unity correspond to disturbances originating within the coating, while values of h greater than unity correspond to disturbances within the fluid.

Values of n are inversely related to the thickness of the transition layer. Figure 4 shows the variation of the real and imaginary part of H (Eq. 19a) for two different values of n .

A value of n equal to 8 thus corresponds to a transition layer starting at $y/\ell = 0.75$ and ending at about $y/\ell = 1.35$. The transition layer is thus seen to be about equal in thickness as the main coating itself. A value of n equal to 32 instead corresponds to a transition layer starting at $y/\ell = 0.95$ and ending at $y/\ell = 1.05$; the thickness of the transition layer is thus equal to 10% of the compliant coating. The transition

layer has been defined as starting where the value of the real part of H is less than 90% of its value within the compliant coating. In a similar manner, the outer edge of the transition layer is defined to be the point where the value of the imaginary part of H is within 10% of the fluid value. The point where the real part of H equals the imaginary part is the location where the transition layer switches behavior, from solid-like to fluid-like.

Very rigid coatings with relatively large shear moduli will give rise to smaller values of the parameter R than softer coatings. The value of Γ , being linearly related to the dimensional coating thickness " l " will also give an indication of the relative magnitude of the thickness of the coating. As it can be verified by the corresponding definition of both R and Γ , higher frequencies for the disturbance will result in a simultaneous increase in both parameters. Table I gives typical values for frequencies, coating thickness and shear wave speed of the coating for the range of values of R and Γ considered in this report.

$R = 10^{-9}$	$c_s = 2500 \text{ m/s} \text{ --- } f = 10^3 \text{ Hz}$
	$c_s = 250 \text{ m/s} \text{ --- } f = 10 \text{ Hz}$
$R = 10^{-7}$	$c_s = 250 \text{ m/s} \text{ --- } f = 10^3 \text{ Hz}$
	$c_s = 25 \text{ m/s} \text{ --- } f = 10 \text{ Hz}$
$R = 10^{-5}$	$c_s = 25 \text{ m/s} \text{ --- } f = 10^3 \text{ Hz}$
	$c_s = 2.5 \text{ m/s} \text{ --- } f = 10 \text{ Hz}$
$\Gamma = 10$	$f = 10^3 \text{ Hz} \text{ --- } l = 0.25 \text{ mm}$
	$f = 10 \text{ Hz} \text{ --- } l = 1.25 \text{ mm}$
$\Gamma = 10^2$	$f = 10^3 \text{ Hz} \text{ --- } l = 1.25 \text{ mm}$
	$f = 10 \text{ Hz} \text{ --- } l = 12.5 \text{ mm}$
$\Gamma = 10^3$	$f = 10^3 \text{ Hz} \text{ --- } l = 1.25 \text{ cm}$
	$f = 10 \text{ Hz} \text{ --- } l = 12.5 \text{ cm}$

Table 1 - Typical Values of R and Γ for
and Elastic-Coating-Water System.

The results of the numerical integration of the differential equation are presented in terms of particle displacement $|u|$, local shear stress $|\tau|$ and local power distribution $|P|$ for the different parameters (n, h, R, Γ) considered. The power transmitted from the location of the disturbance to any point of interest is obtained from the definition

$$P = \int_0^T \tau \, du \quad , \quad (28)$$

where the integral is over one cycle of the disturbance and τ and u are the local shear stress and particle displacement respectively. Noting that

$$\tau = \tau(y) \exp(-i\omega t) \quad , \quad (29)$$

$$du = v \, dt = -i\omega u \, dt \quad , \quad (30)$$

$$T = 1/f \quad , \quad (31)$$

equation 28 can be written as

$$P = \tau(y) u(y) \quad . \quad (32)$$

Figures 5-7 show the particle displacement distribution for different location, h , of the disturbance and for three values of Γ . Only the profiles from the wall to the disturbance is shown. Values of h less than unity correspond to disturbances within the solid. The displacement distribution for all points within the solid, as expected, is thus seen to

be linear. For all values of Γ considered, the shear fluid disturbance decays rapidly within the fluid and then once it has passed the transition layer, goes to zero at the wall linearly. Figure 8 shows the same type of result in both the linear and the log scale. The dotted lines shown in each of the figures correspond to the classical solution in the absence of a transition layer. Note that, while in the linear scale, the difference between the two displacement distribution seems negligible, when the results are presented on a log scale, the difference between the results with and without the transition layer is more obvious. Figure 9 shows the effect of the transition layer thickness on the displacement distribution, where it is seen that a 10% transition layer thickness (i.e. $n=32$) will still produce a particle displacement distribution an order of magnitude larger than the classical no transition layer solution. Note that for this particular case the displacement distribution within the solid is about 10 orders of magnitude smaller than the initial value. Figure 10 shows the effect of the elastic layer property R on the displacement distribution and is compared with the classical solution. As in the other cases the coating displacement is magnified by the transition layer.

Figures 11-16 show the shear stress distribution within the transition layer and the compliant coating for the different cases considered. Fig. 11 shows the distribution for

three different source location. The distribution for the transition layer case is equal to the classical analysis up to the point where the visco-elastic layer switches from fluidlike to solid-like; at this point the shear stress suddenly increases by an order of magnitude and it then remains constant to the wall. The magnitude of this shift is dependent upon the thickness of the transition layer. The comparisons between the results with and without the viscoelastic layer depend upon whether in the classical solution the elastic is assumed to exist up to $y=l$ or out to the location where the layer switches from solid-like to fluid-like (i.e. $y=1.37l$ for $R = 10^{-5}$). In either case, the present model is seen to cause larger stresses within the compliant layer. Figure 12 shows the effect of the thickness of the viscoelastic layer. Figures 13 and 14 illustrate the effect of different coating materials for two different layer thicknesses and it is seen that in both instances, the softer compliant coatings (i.e. larger values of R) will result in greater differences between the coating-fluid systems with and without the transition layer. Figures 15 and 16 show the effect of the compliant coating thickness upon the shear stress distribution. From these figures it is seen that the importance of the transition layer is more clear for thicker compliant coatings (i.e. larger values of Γ). The thicker viscoelastic layer, not only causes the sharp reversal in the stress distribution, but under certain conditions, causes a double reversal to develop (see $R=10^{-5}$, $\Gamma=200$ case).

The parameter that determines the magnitude of the

interaction between the fluid and the compliant coating is the amount of power (Eq. 32) transmitted from the fluid into the coating. Figure 17 shows the effect of transition layer thickness on the power level, and figure 18 considers different coating materials. In all cases, the transition layer allows more power to be transmitted into the coating. From the results presented in figure 18 it is seen that while the transmitted power for the no transition layer varies linearly as a function of R , the presence of the transition layer reduces the dependence to about $R^{1/2}$.

Figures 19 and 20 compare the exponentially varying transition layer inhomogeneity with a linear inhomogeneity with the same end conditions. A stress driven fluid disturbance propagating into the coating is shown in figure 21 and 22 and as expected it is seen to have exactly the same distribution as the displacement driven disturbance. This latter result is as expected from the reciprocal theorem of linear media.

The results by Pedersen et al³ are in general agreement with the results obtained in this report.

IV. CONCLUSION

In this present analysis, the interaction between a fluid transverse disturbance, a purely elastic compliant coating and an inhomogeneous transition layer at the interface has been studied. The fluid disturbance has been assumed to take place in the absence of a mean flow field, and either a transverse displacement or a shear stress have been assumed to be one dimensional in space and sinusoidal in time.

The results obtained in this report, have shown that a thin viscoelastic inhomogeneous layer can radically alter the interaction between a fluid shear disturbance and a compliant surface. Depending upon the coating and the transition layer thickness as well as the frequency of oscillation, the presence of the transition layer lets a greater amount of energy into the coating.

Although, to more fully understand the interaction mechanism, the compliant coating was assumed to be purely elastic, the results can be carried over to the case of a damped coating. The transition layer will allow more of the energy into the coating which would then be absorbed.

The inhomogeneity of the layer can be thought as being due to one or more of four possibilities: (1) layer with continuously varying conditions, (2) a series of thinner homogeneous layers each having different properties, (3) the coating is hydrophobic (4) the coating, being forced in a random manner by

the fluid effectively spreads out the discontinuities of the interface into a layer with finite thickness.

The greater percentage of power transfer from the fluid into the coating, achieved by means of a transition layer may stimulate new ideas which could lead to more successful compliant coatings.

V. REFERENCES

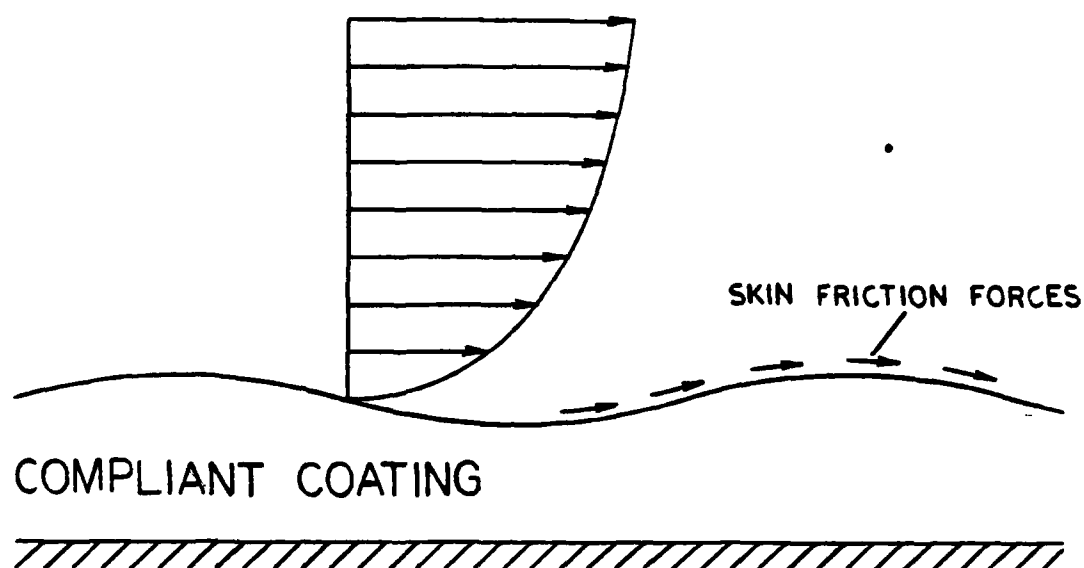
1. M. Pierucci, P. A. Baxley, "Compliant-Coating-Fluid Interaction: Coating Shear Waves in Stationary Fluid" AE&EM TR-82-03, San Diego State University, February 1982.
2. M. Pierucci, P. A. Baxley, "Compliant Coating-Fluid Interaction: Coating Longitudinal Waves in Stationary Fluid", AE&EM TR-82-04, San Diego State University, February 1982.
3. P. C. Pedersen, O. Tretiak, P. He, "Impedance-Matching Properties of an Inhomogeneous Matching Layer with Continuously Changing Acoustic Impedance, "J. Acoust. Soc. Am. 72, 327-336, 1982.

List of Figures

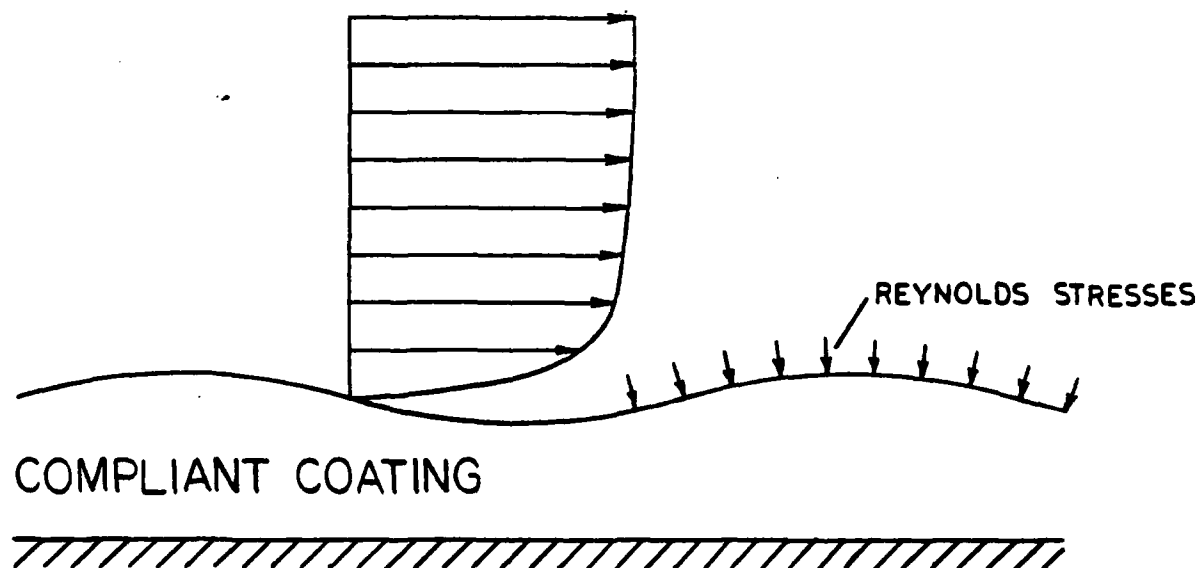
- Fig. 1.** Compliant-Coating-Boundary-Layer-Interaction.
(a) Laminar Boundary Layer; (b) Turbulent Boundary Layer.
- Fig. 2.** Transition Layer Models. (a) Viscoelastic Inhomogeneous Layer; (b) Equivalent Transition Layer Due to Surface Motion.
- Fig. 3.** Variation of the Stress-Strain Coefficient as a Function of Wall Distance for (a) No transition, (b) Inhomogeneous Transition Layer.
- Fig. 4.** Typical Transition Layer Property. $H = e^{-(y/l)^n} - 1R(1 - e^{-(y/l)^n})$. $R = 10^{-5}$.
- Fig. 5.** Particle Displacement Distribution. Effects of Location of Disturbance. $R = 10^{-5}$, $\Gamma = 10$, $n=8$.----- No Transition Layer.
- Fig. 6.** Particle Displacement Distribution. Effect of Location of Disturbance. $R = 10^{-5}$, $\Gamma = 50$, $n = 8$.
- Fig. 7.** Particle Displacement Distribution. Effect of Location of Disturbance. $R = 10^{-5}$, $\Gamma = 200$, $n = 8$.
- Fig. 8.** Typical Particle Displacement Distribution. $R = 10^{-5}$, $n = 32$, $h = 1.25$. (a) Linear Scale; (b) Log Scale.----- No Transition Layer.
- Fig. 9.** Effect of Transition Layer Thickness on Particle Displacement Distribution. $R = 10^{-5}$, $\Gamma = 50$, $h = 1.5$.----- No Transition Layer.

- Fig. 10. Effect of Coating Property R on particle Displacement Distribution. $\Gamma = 200$, $h = 1.25$, $n = 32$.
- Fig. 11. Local Shear Stress Distribution Due to a Unit Shear Disturbance at Three Different Locations. $R = 10^{-5}$, $\Gamma = 50$, $n = 8$. ---- Interface at $y = \ell$. ——— Interface at y value where $H_r = H_i$.
- Fig. 12. Local Shear Stress Distribution for three Different Transition Layers. $R = 10^{-5}$, $\Gamma = 50$, $h = 1.5$. ---- No Transition Layer.
- Fig. 13. Effect of Coating Properties on Shear Stress Distribution. $n=8$, $\Gamma = 200$, $h = 1.5$. ---- No transition Layer, Interface at $y = \ell$, ——— No transition Layer, Interface at Point Where $H_r = H_i$.
- Fig. 14. Effect of Elastic Layer Properties on Shear Stress Distribution. $N = 32$, $\ell = 200$, $h = 1.25$. ----- No Transition Layer, Interface at $y = \ell$. ——— - ——— No Transition Layer, Interface at Point where $H_r = H_i$.
- Fig. 15. Effect of Coating Thickness Parameter on Local Shear Stress Distribution. $R = 10^{-5}$, $n = 8$, $h = 1.5$.
- Fig. 16. Effect of Coating Thickness Parameter Γ on Local Shear Stress Distribution. $R = 10^{-5}$, $n = 32$, $h = 1.25$. ----- No Transition Layer.

- Fig. 17. Non-Dimensional Power Level Distribution as a Function of Transition Layer Thickness. $\Gamma = 50$, $R = 10^{-5}$, $h = 1.5$. ---- No Transition Layer.
- Fig. 18. Non-Dimensional Power Level Distribution for Different Coating Parameters R . $\Gamma = 200$, $n = 32$, $n = 1.25$. ---- No Transition Layer.
- Fig. 19. Comparison of Particle Displacement Distribution for the Exponential and the Linear Inhomogeneity. $R = 10^{-5}$, $\Gamma = 50$, $n = 32$, $h = 1.25$. ——— Exponential Inhomogeneity. ---- Linear Inhomogeneity.
- Fig. 20. Comparison of Shear Stress Distribution for the Exponential and the Linear Inhomogeneity. $R = 10^{-5}$, $\Gamma = 50$, $n = 32$, $h = 1.25$. ——— Exponential Inhomogeneity. ---- Linear Inhomogeneity.
- Fig. 21. Particle Displacement Distribution for a Stress-Driven Shear Disturbance. $R = 10^{-5}$, $\Gamma = 50$, $h = 1.25$, $n = 32$.
- Fig. 22. Stress Distribution for a Stress-Driven Shear Disturbance. $R = 10^{-5}$, $\Gamma = 50$, $h = 1.25$, $n = 32$.

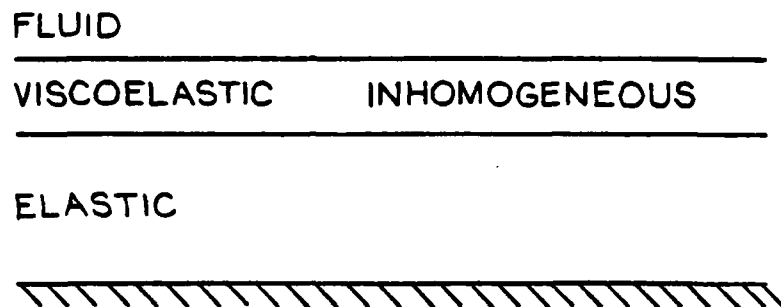


(a)

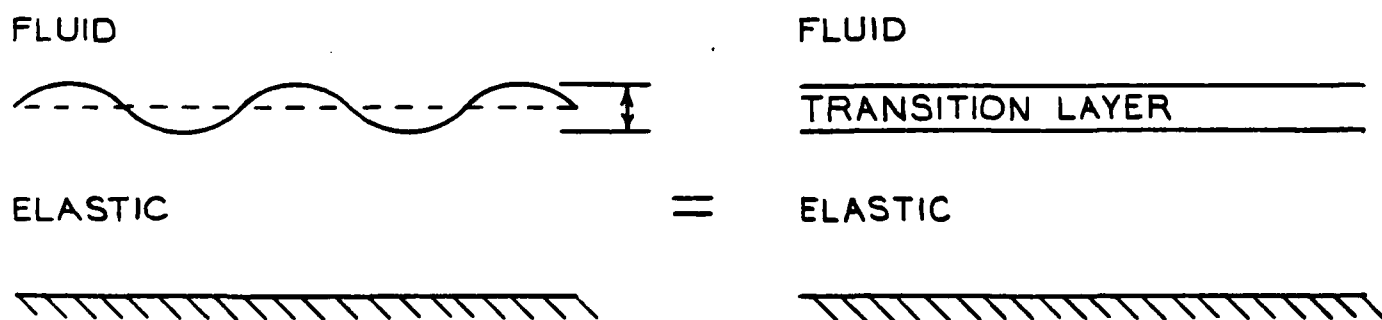


(b)

Fig. 1. Compliant-Coating-Boundary-Layer-Interaction. (a) Laminar Boundary Layer; (b) Turbulent Boundary Layer.

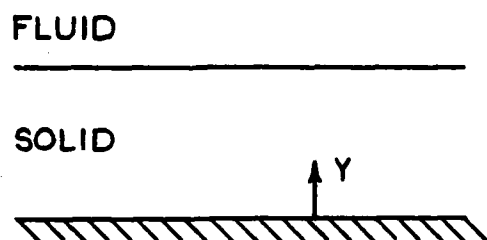


(a)

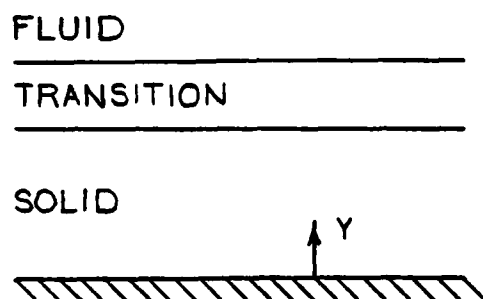
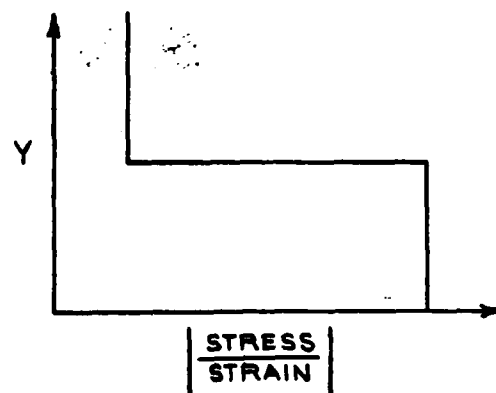


(b)

Fig. 2. Transition Layer Models. (a) Viscoelastic Inhomogeneous Layer; (b) Equivalent Transition Layer Due to Surface Motion.



(a)



(b)

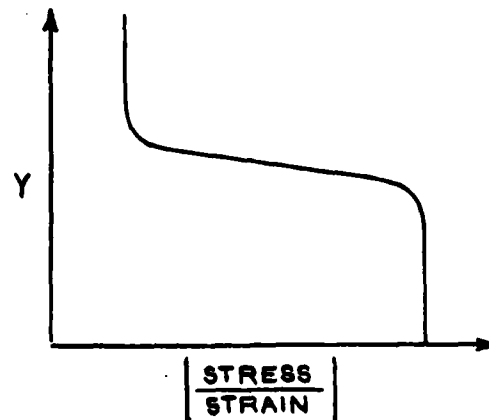


Fig. 3. Variation of the Stress-Strain Coefficient as a Function of Wall Distance for (a) No Transition, (b) Inhomogeneous Transition Layer.

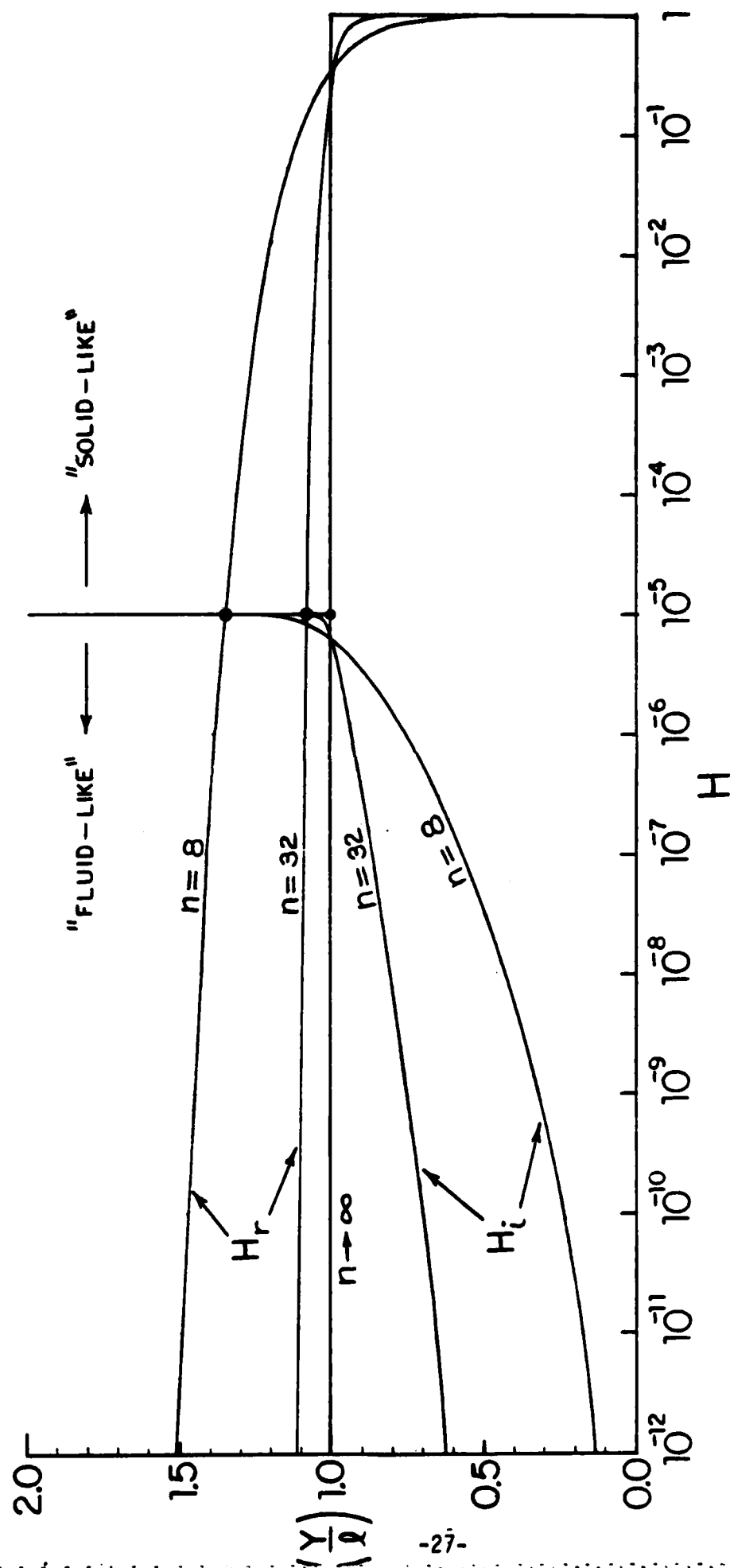


Fig. 4. Typical Transition Layer Property. $H = e^{-(y/l)^n} - iR(1 - e^{-(y/l)^n})$. $R = 10^{-5}$.

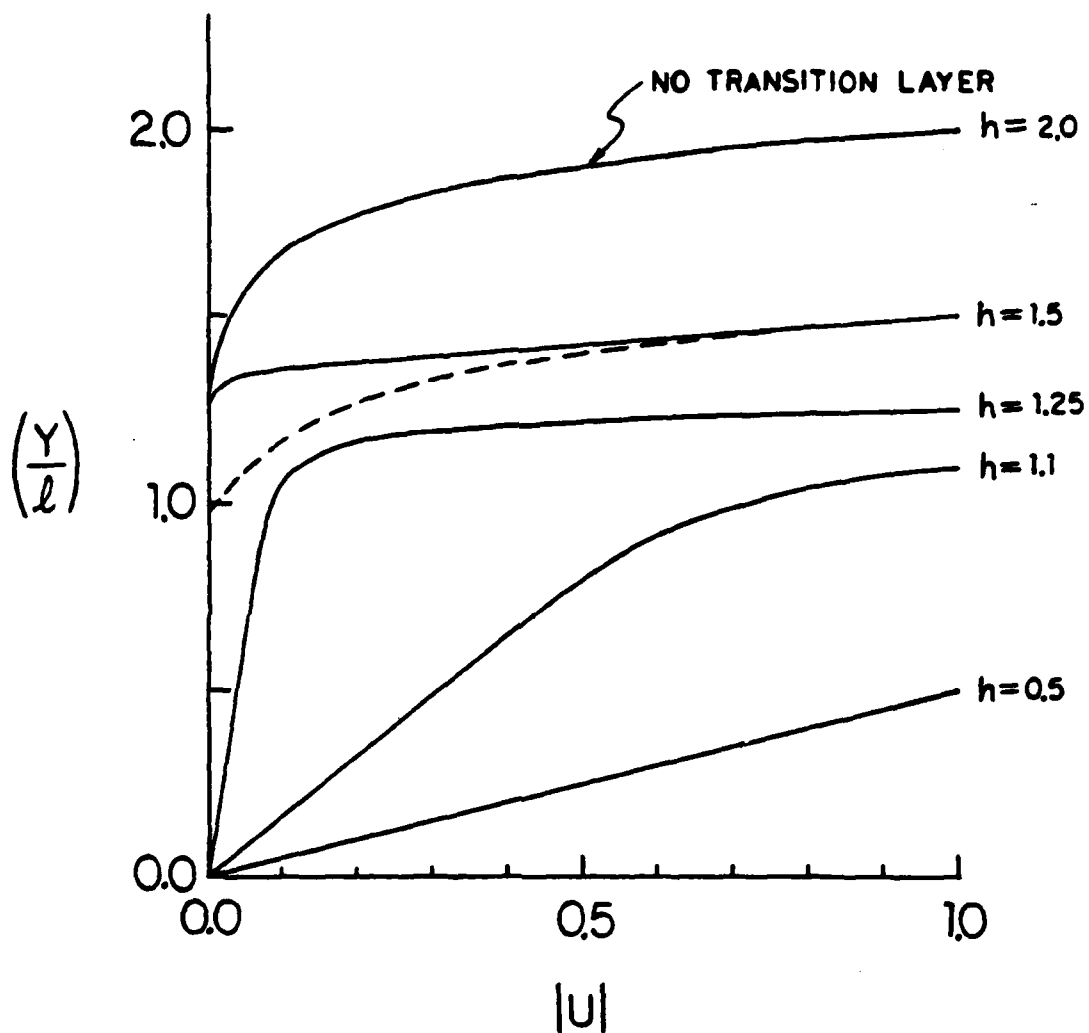


Fig. 5. Particle Displacement Distribution. Effects of Location of Disturbance. $R = 10^{-5}$, $\Gamma = 10$, $n = 8$. ---- No Transition Layer.

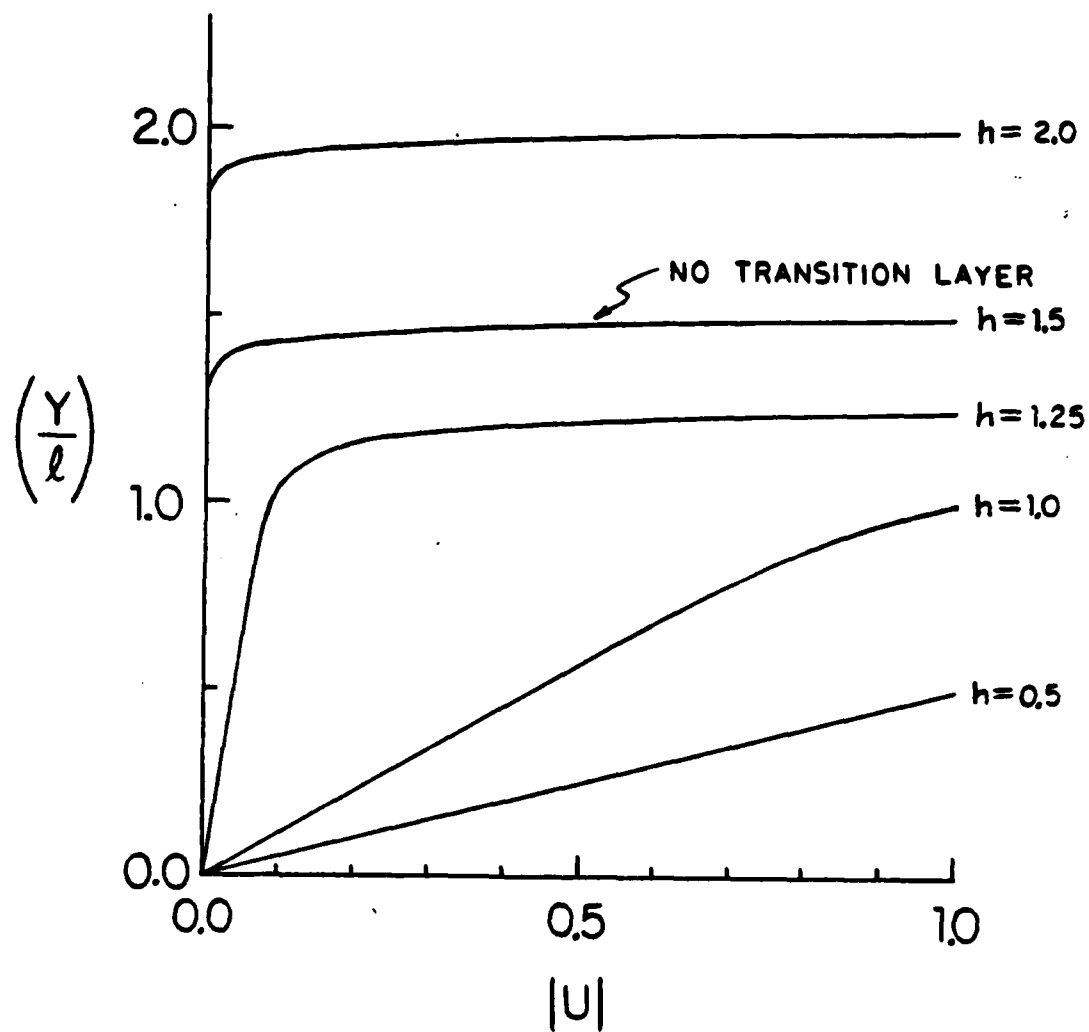


Fig. 6. Particle Displacement Distribution. Effect of Location of Disturbance. $R = 10^{-5}$, $T = 50$, $n = 8$.

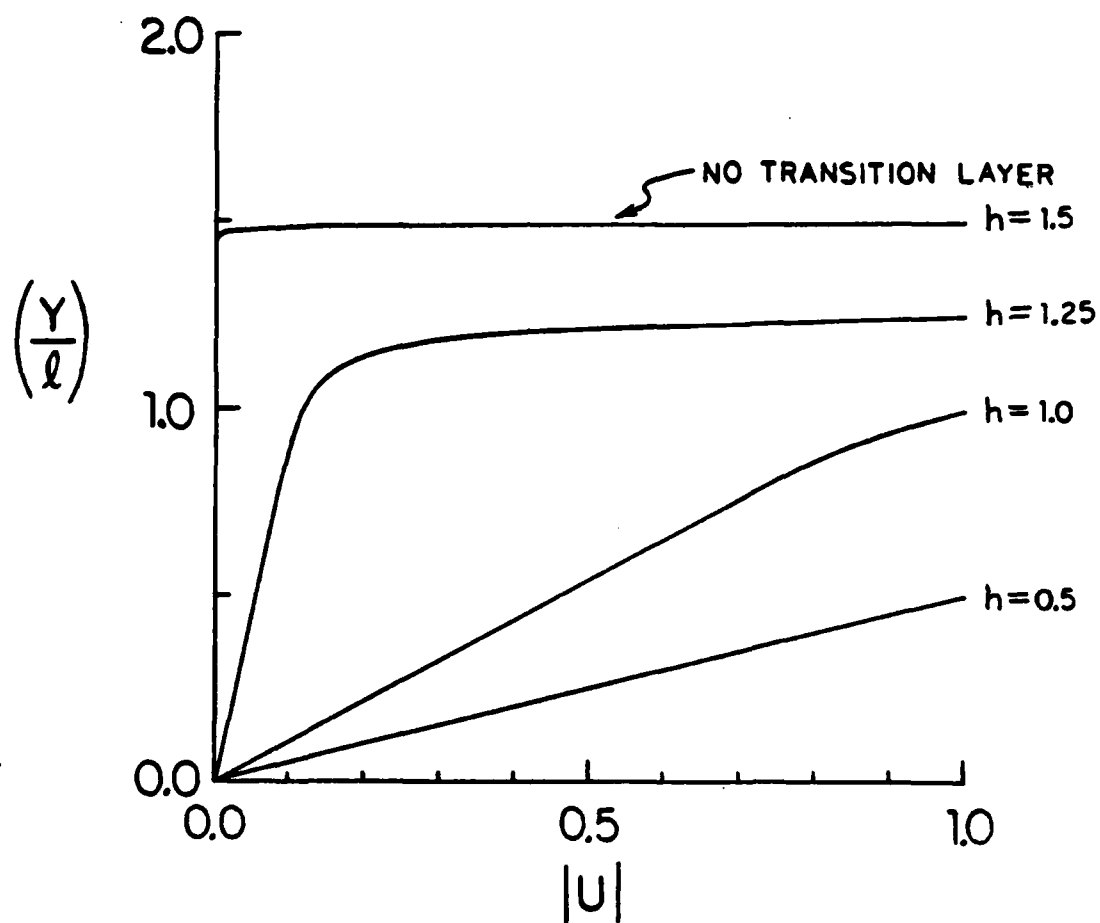


Fig. 7. Particle Displacement Distribution. Effect of Location of Disturbance. $R = 10^{-5}$, $\Gamma = 200$, $n = 8$.

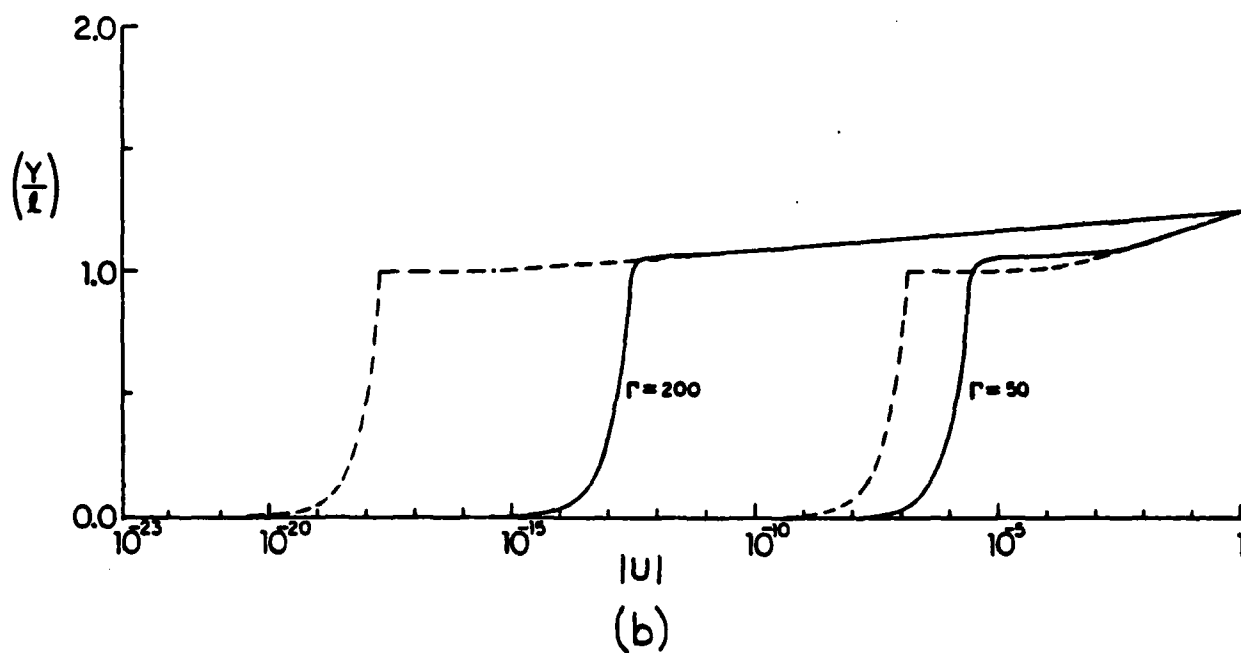
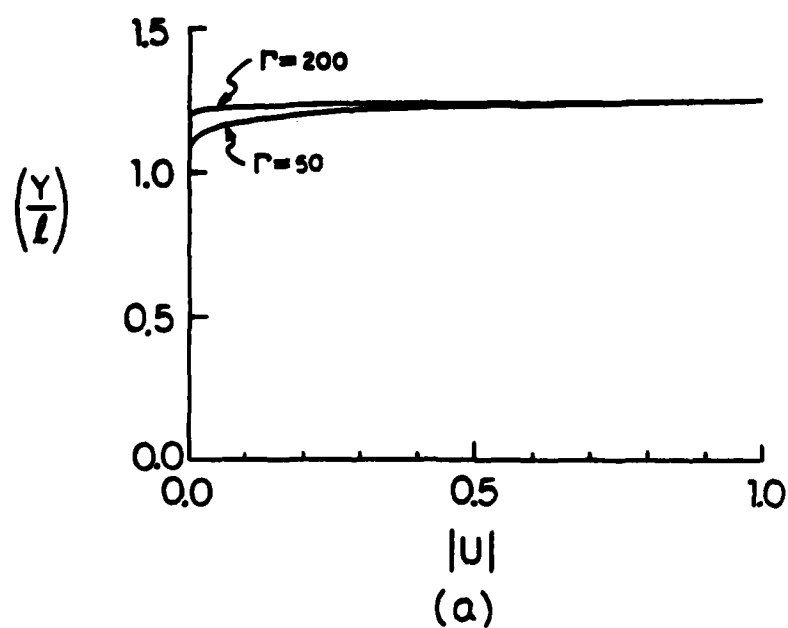


Fig. 8. Typical Particle Displacement Distribution. $R = 10^{-5}$, $n = 32$, $h = 1.25$.
 (a) Linear Scale; (b) Log Scale. ----- No Transition Layer.

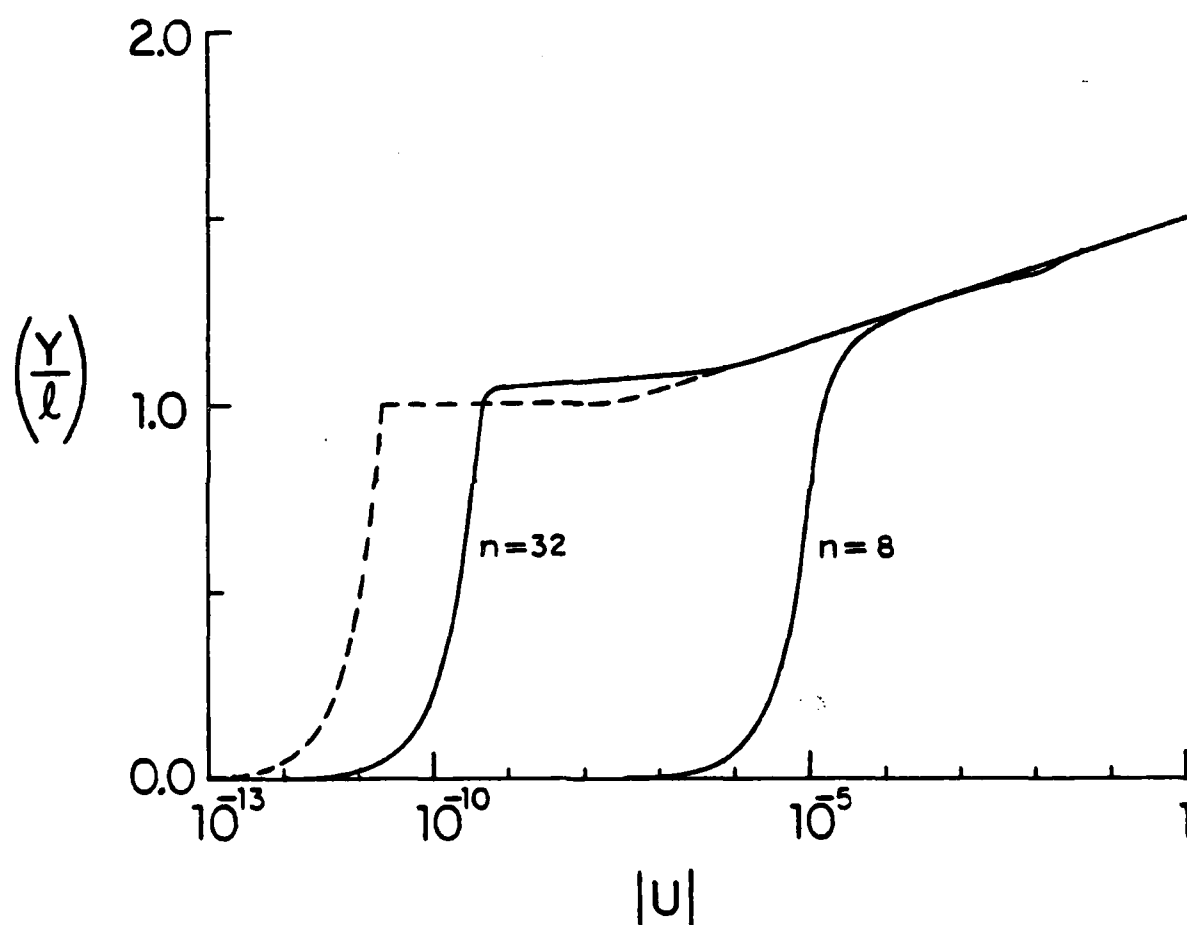


Fig. 9. Effect of Transition Layer Thickness on Particle Displacement Distribution. $R = 10^{-5}$, $\Gamma = 50$, $h = 1.5$. ----- No Transition Layer.

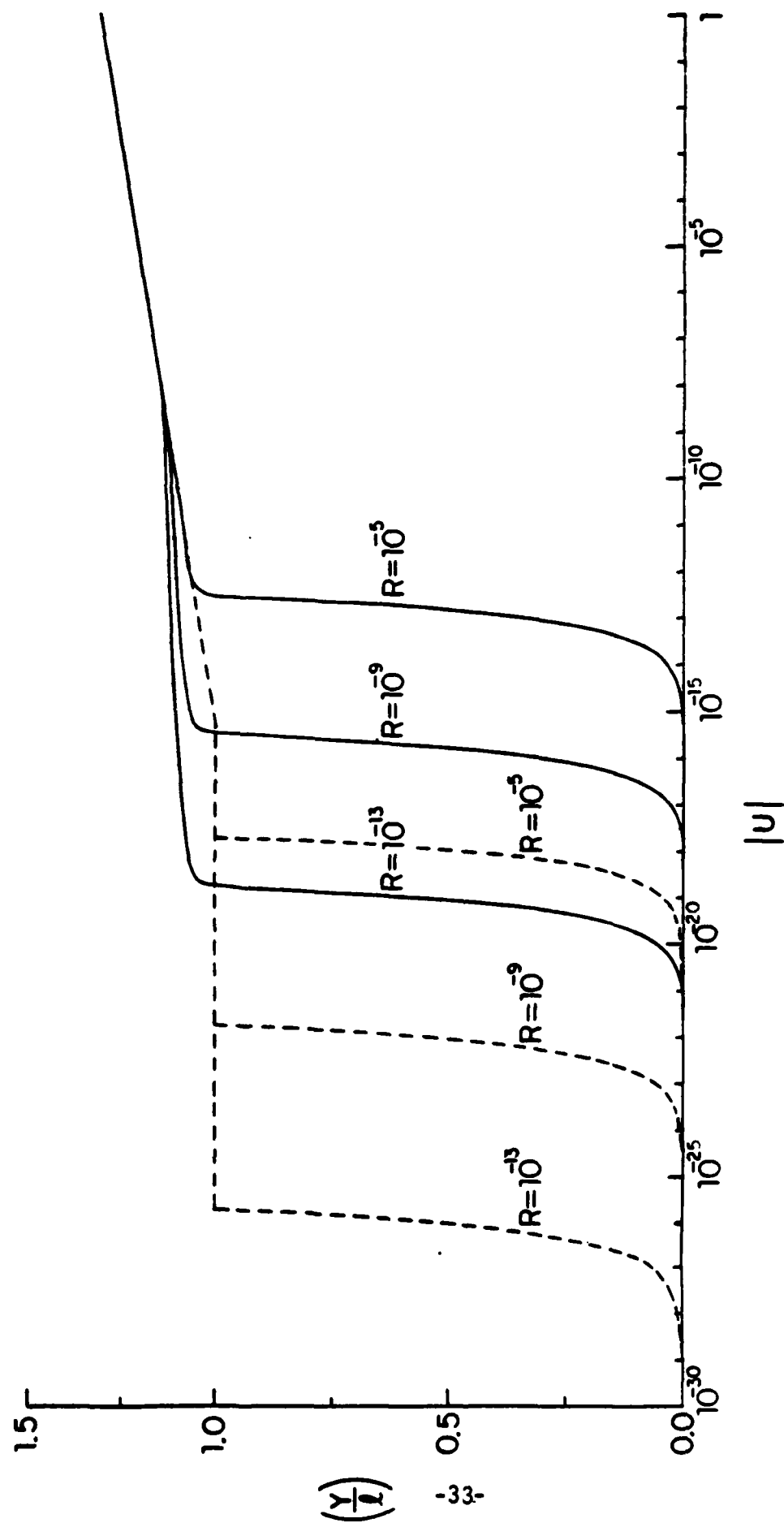


Fig. 10. Effect of Coating Property R on Particle Displacement Distribution. $\Gamma = 200$, $h = 1.25$, $n = 32$.

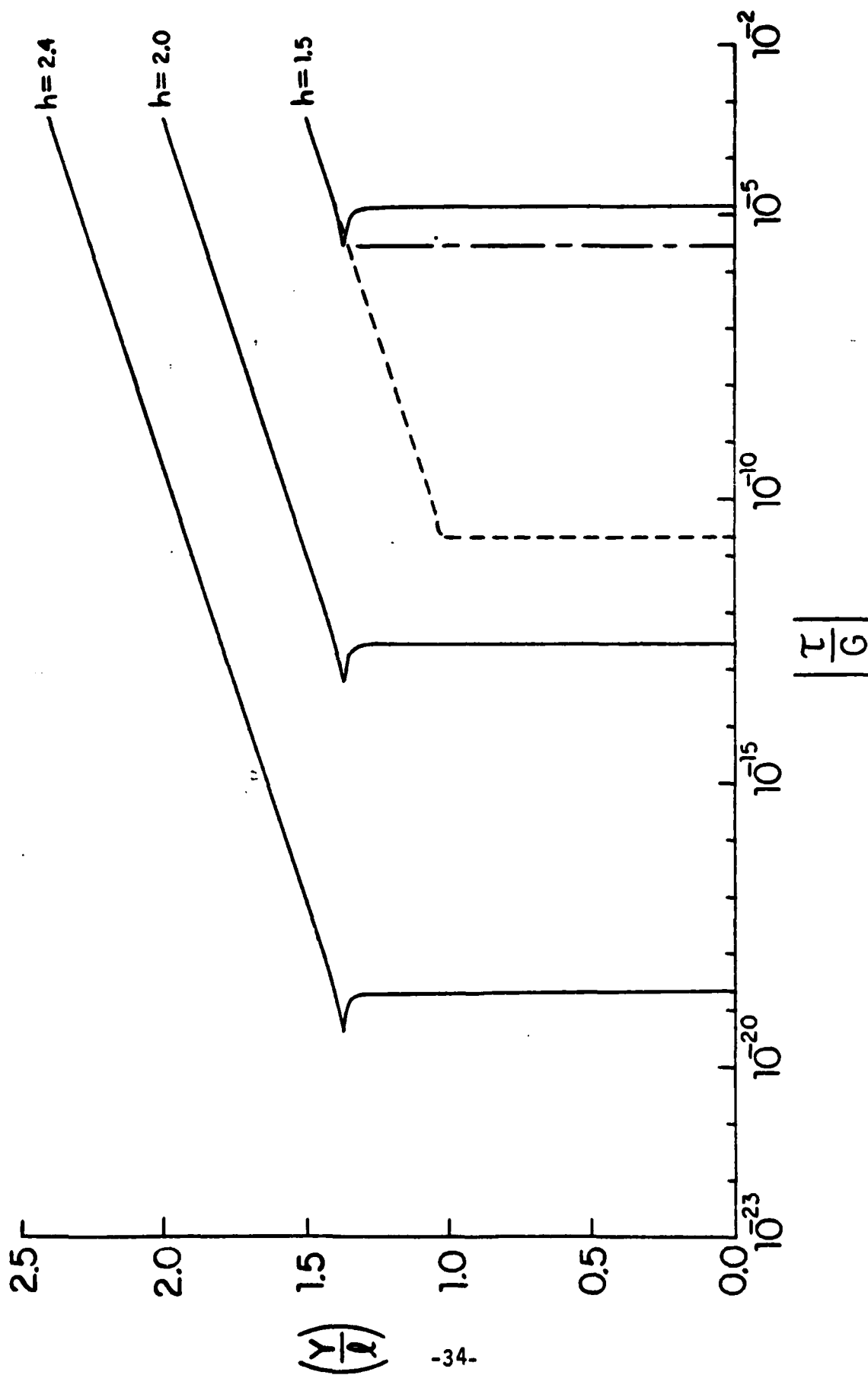


Fig. 11. Local Shear Stress Distribution Due to a Unit Shear Disturbance at Three Different Locations.
 $R = 10^{-5}$, $\Gamma = 50$, $n = 8$. ---- Interface at $y = l$. - - - - Interface at $y = 8$.
 Where $H_j = H_j$.

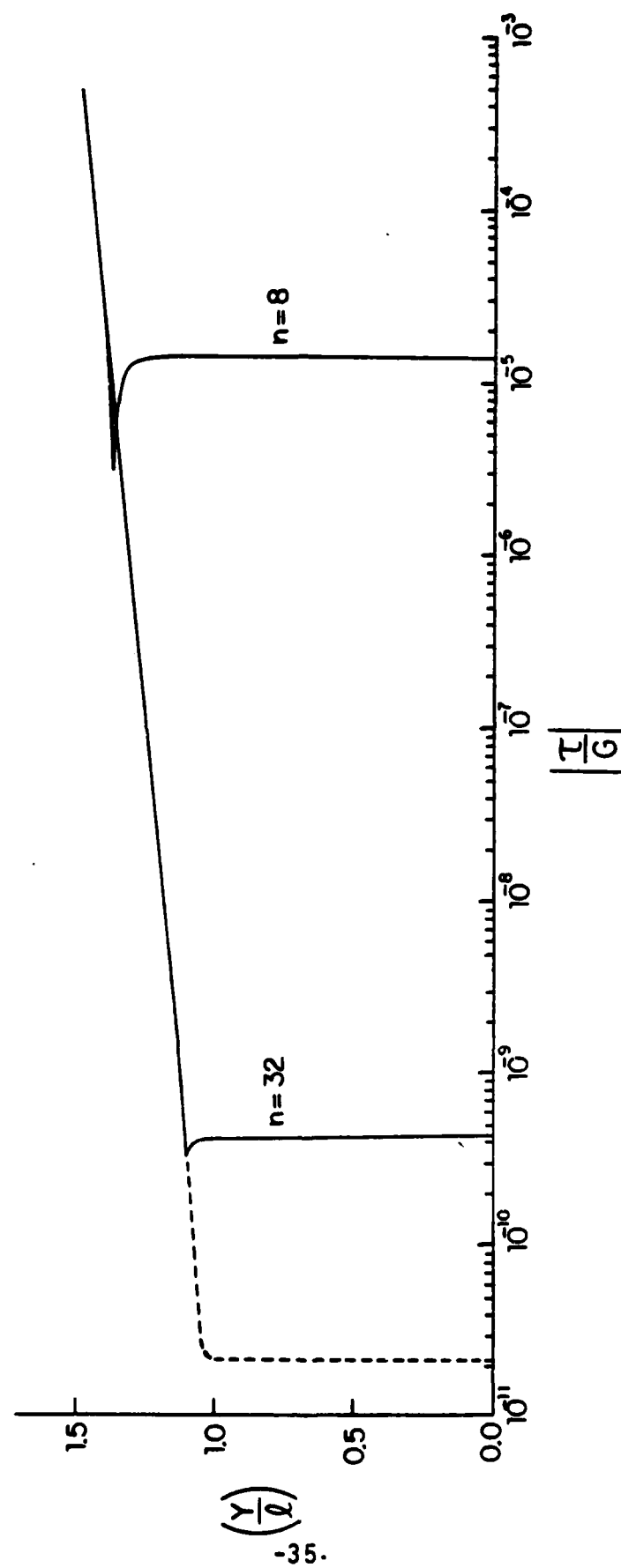


Fig. 12. Local Shear Stress Distribution for Three Different Transition Layers. $R = 10^{-5}$, $\Gamma = 50$, $h = 1.5$. ----- No Transition Layer.

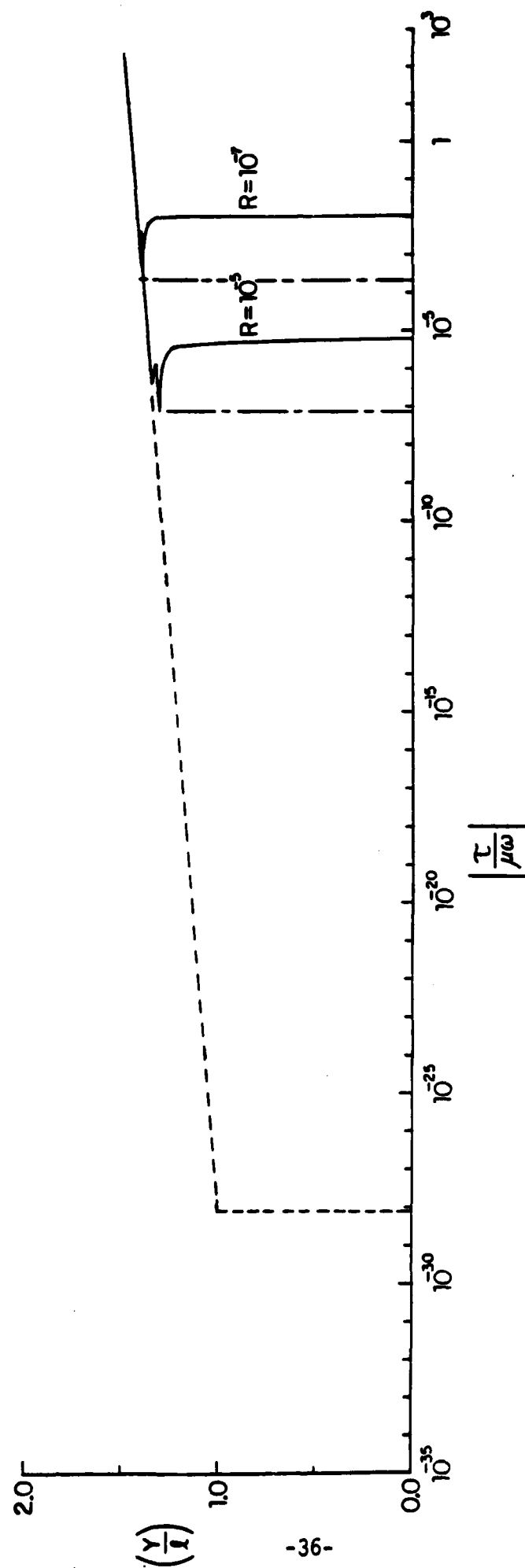


Fig. 13. Effect of Coating Properties on Shear Stress Distribution. $n = 8$, $\Gamma = 200$, $h = 1.5$. ---- No Transition Layer, Interface at $y = l$. ——— No Transition Layer, Interface at Point Where $H_T = H_I$.

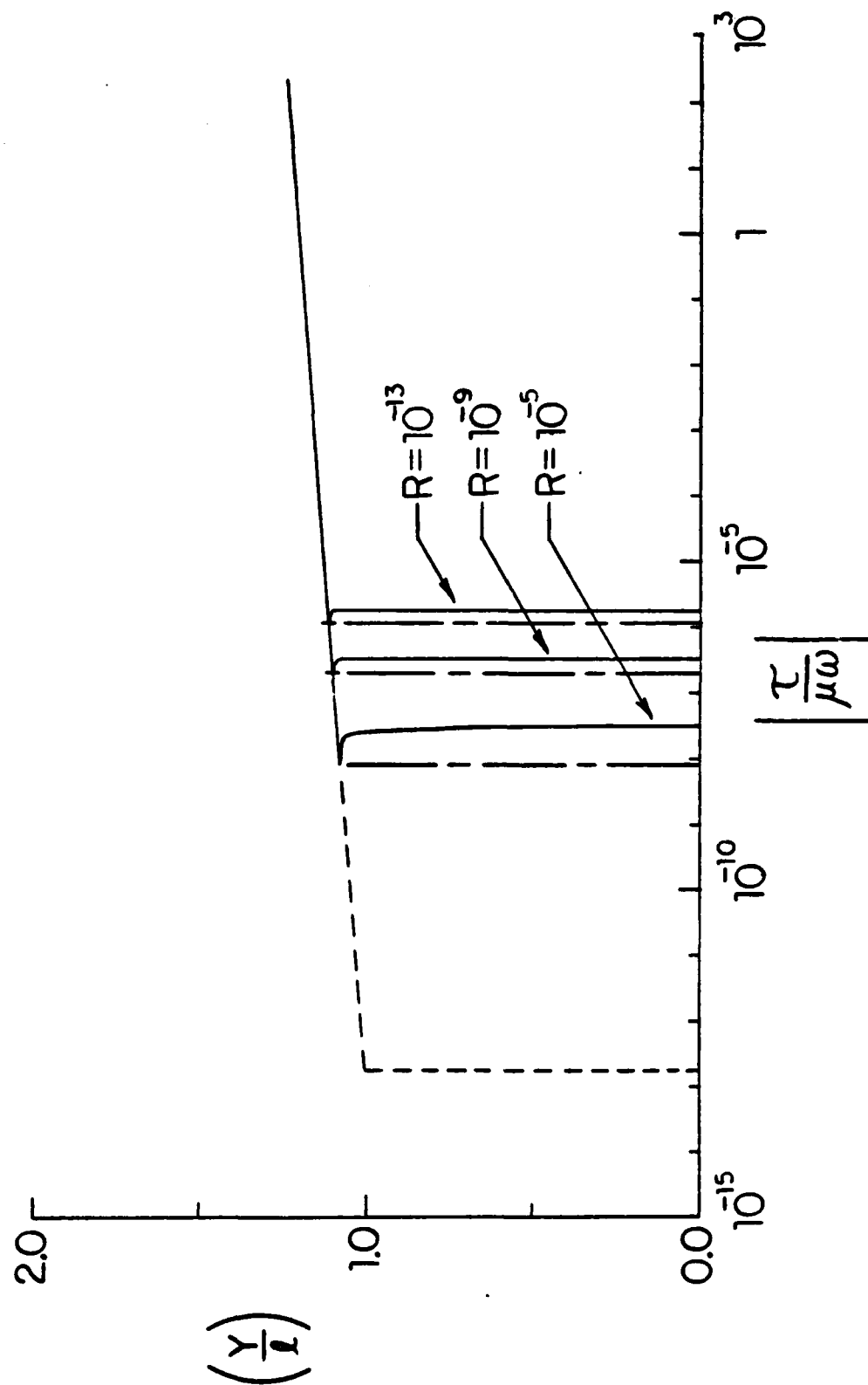


Fig. 14. Effect of Elastic Layer Properties on Shear Stress Distribution. $n = 32$, $\Gamma = 200$, $h = 1.25$.
 ----- No Transition Layer, Interface at $y = l$. ——— No Transition Layer, Interface at Point where $H_r = H_j$.

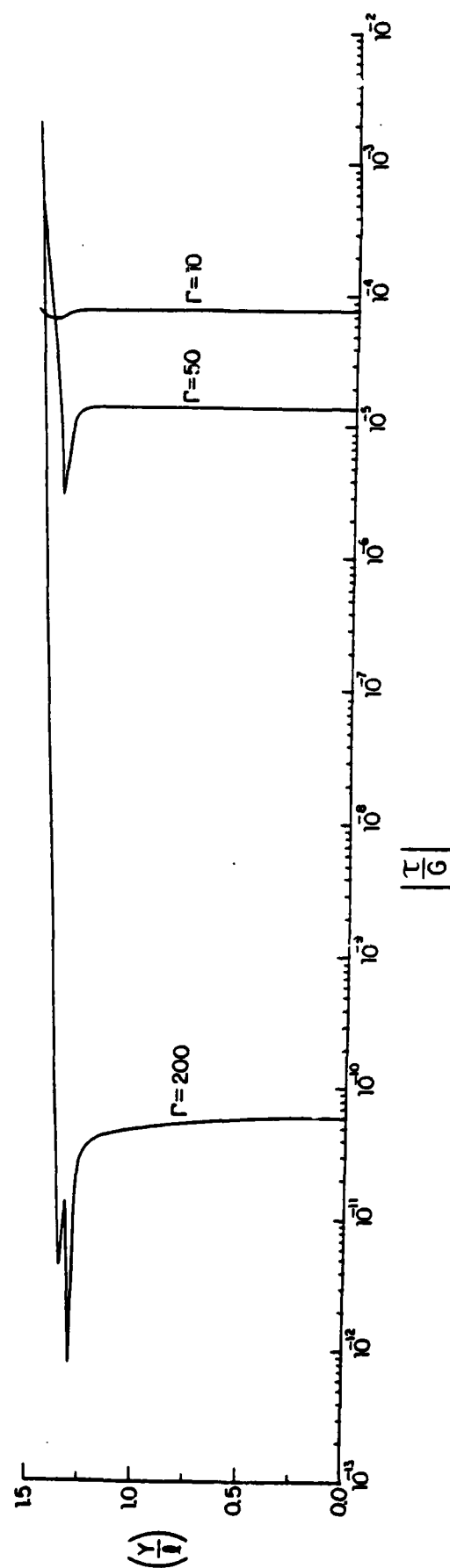


Fig. 15. Effect of Coating Thickness Parameter Γ on Local Shear Stress Distribution. $R = 10^{-5}$, $n = 8$, $h = 1.5$.

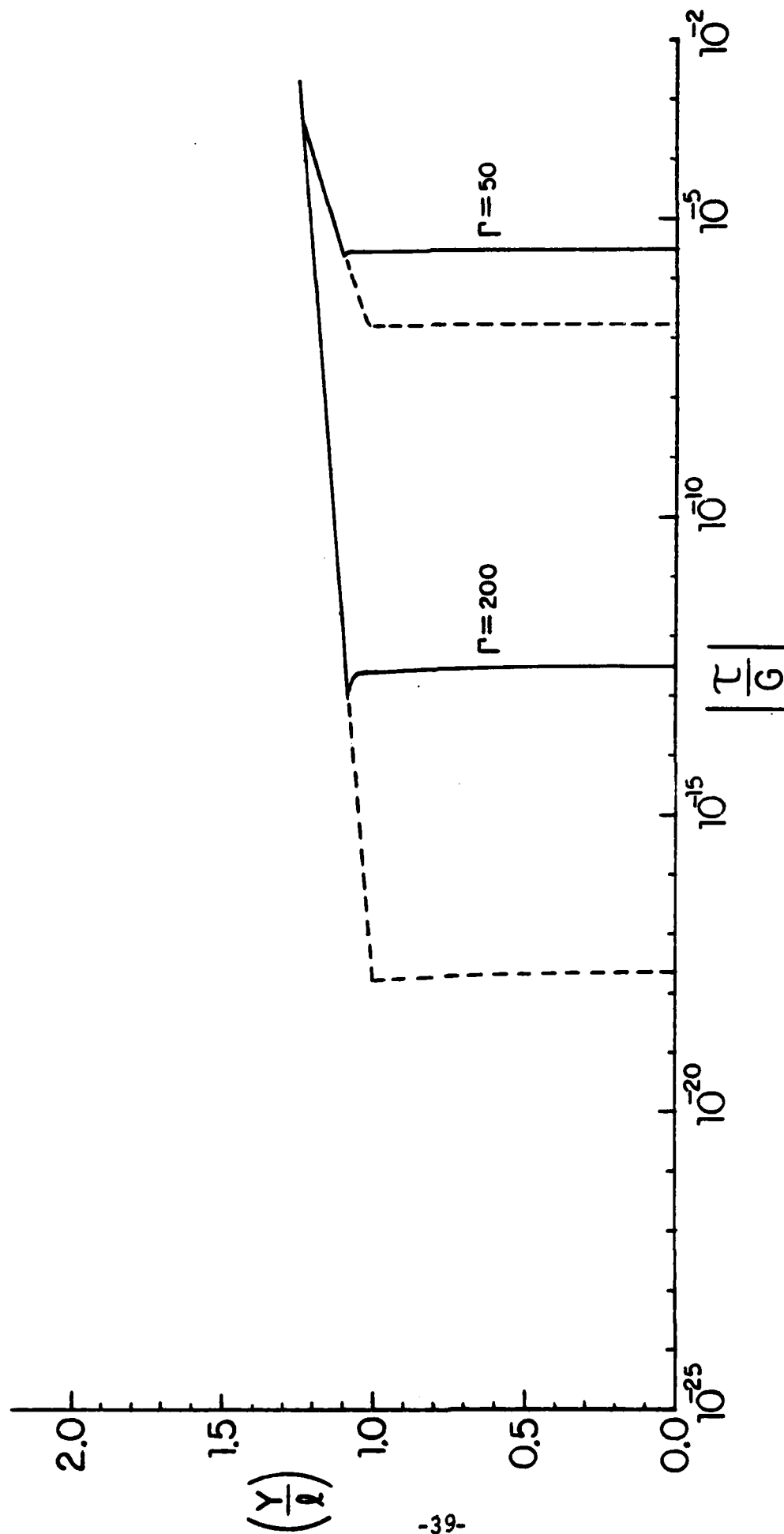


Fig. 16. Effect of Coating Thickness Parameter Γ on Local Shear Stress Distribution. $R = 10^{-5}$, $n = 32$, $h = 1.25$.
 ---- No Transition Layer.

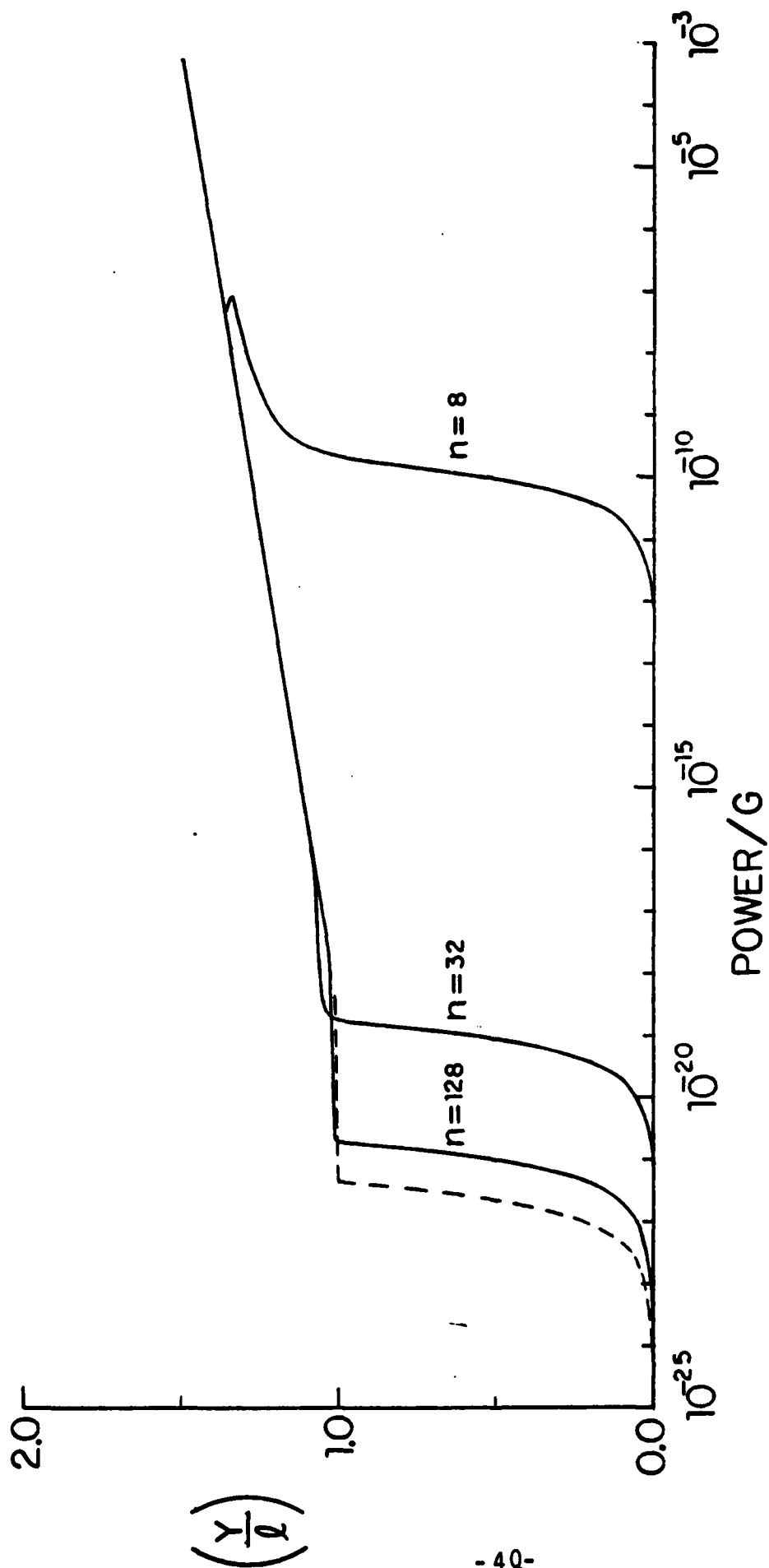


Fig. 17. Non-Dimensional Power Level Distribution as a Function of Transition Layer Thickness. $\Gamma = 50$, $R = 10^{-5}$, $h = 1.5$. ---- No Transition Layer.

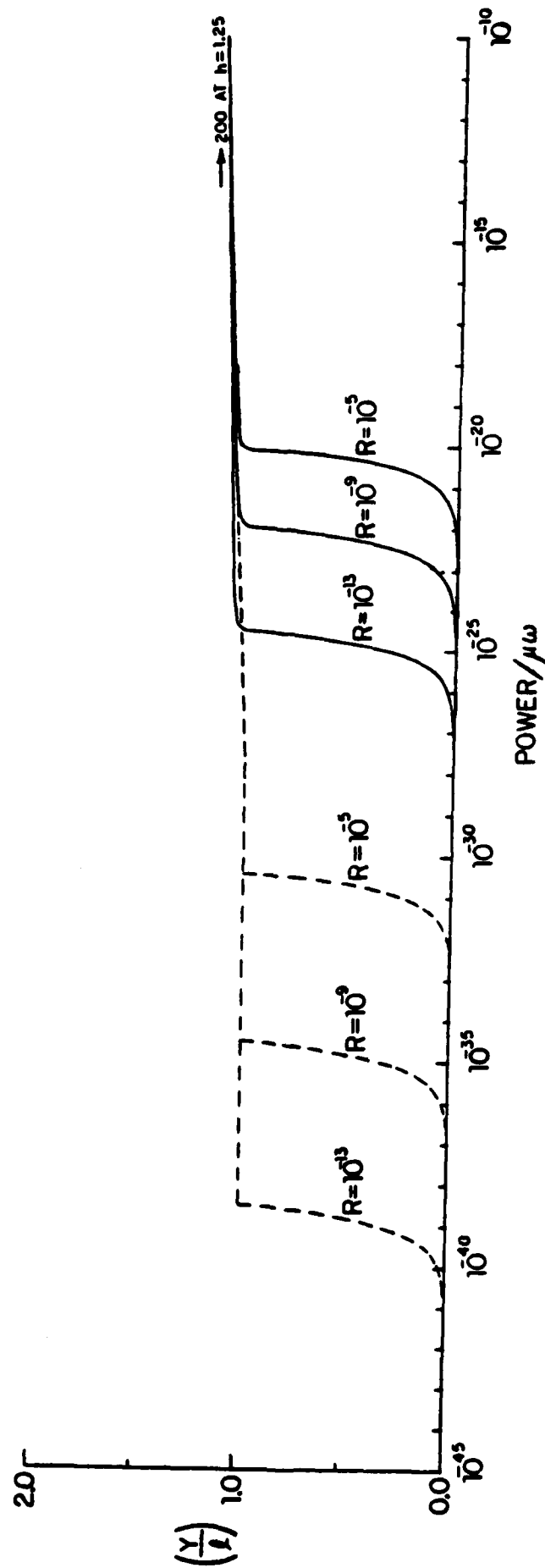


Fig. 18. Non-Dimensional Power Level Distribution for Different Coating Parameters R . $\Gamma = 200$, $n = 32$, $h = 1.25$.
 ----- No Transition Layer.

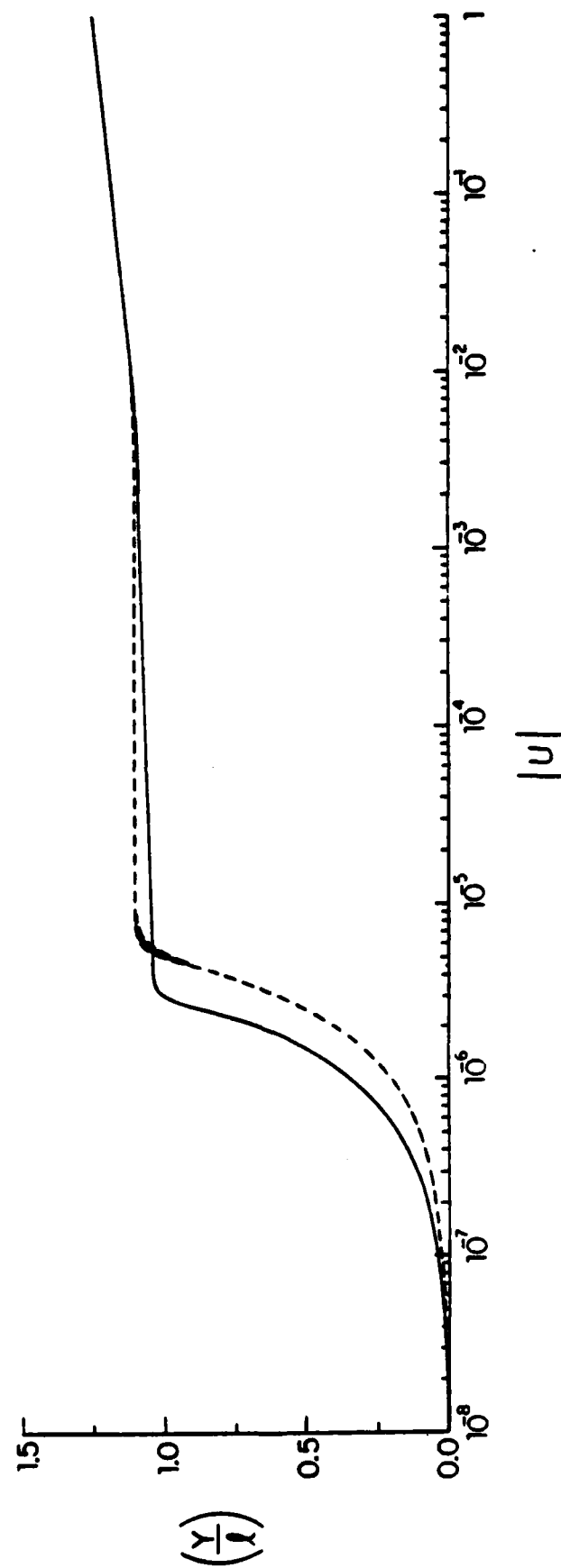


Fig. 19. Comparison of Particle Displacement Distribution for the Exponential and the Linear Inhomogeneity. $R = 10^{-5}$, $\Gamma = 50$, $n = 32$, $h = 1.25$. — Exponential Inhomogeneity. ---- Linear Inhomogeneity.

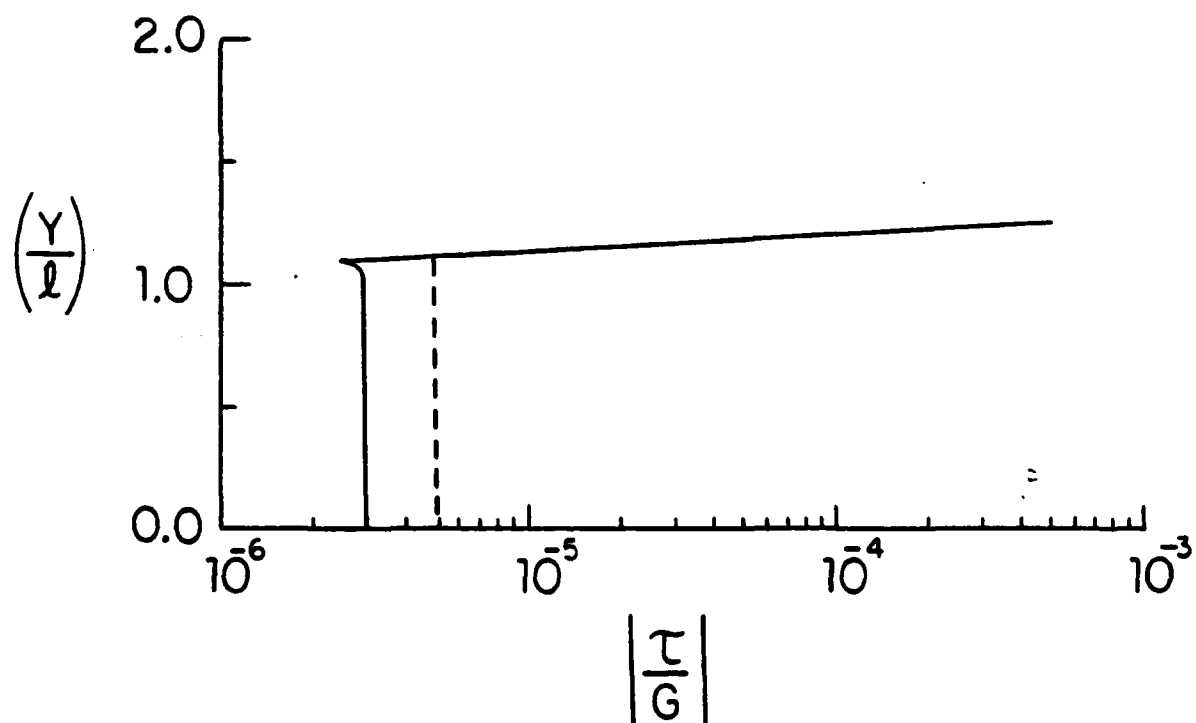


Fig. 20. Comparison of Shear Stress Distribution for the Exponential and the Linear Inhomogeneity. $R = 10^{-5}$, $\Gamma = 50$, $n = 32$, $h = 1.25$. — Exponential Inhomogeneity. ---- Linear Inhomogeneity.

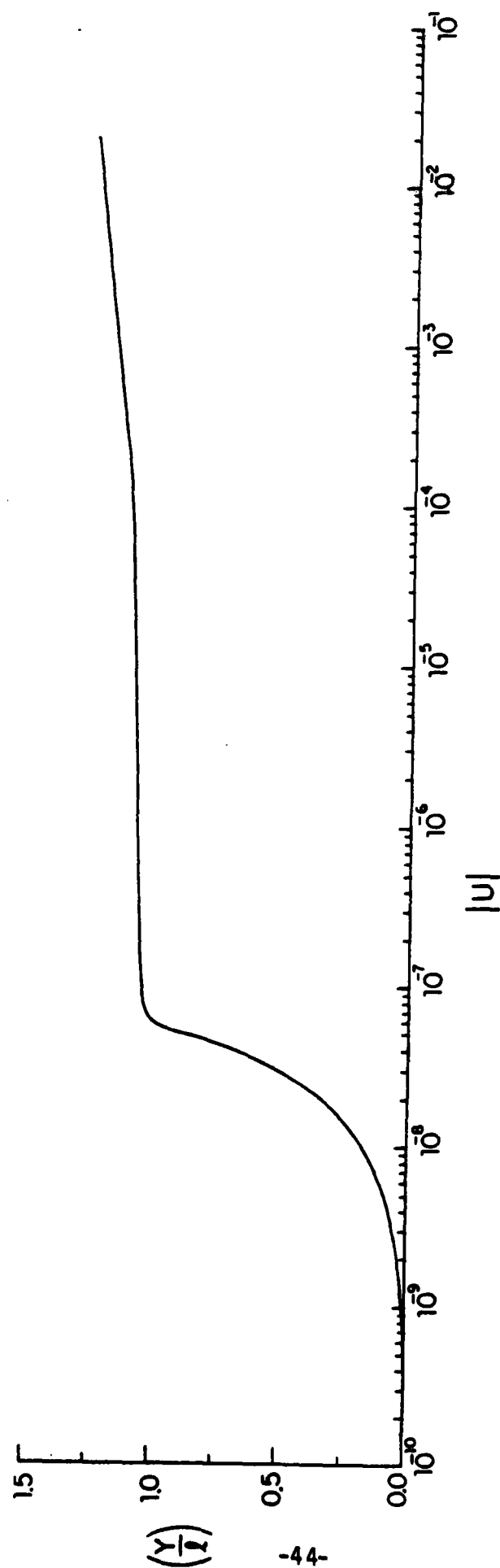


Fig. 21. Particle Displacement Distribution for a Stress-Driven Shear Disturbance. $R = 10^{-5}$, $\Gamma = 50$, $h = 1.25$, $n = 32$.

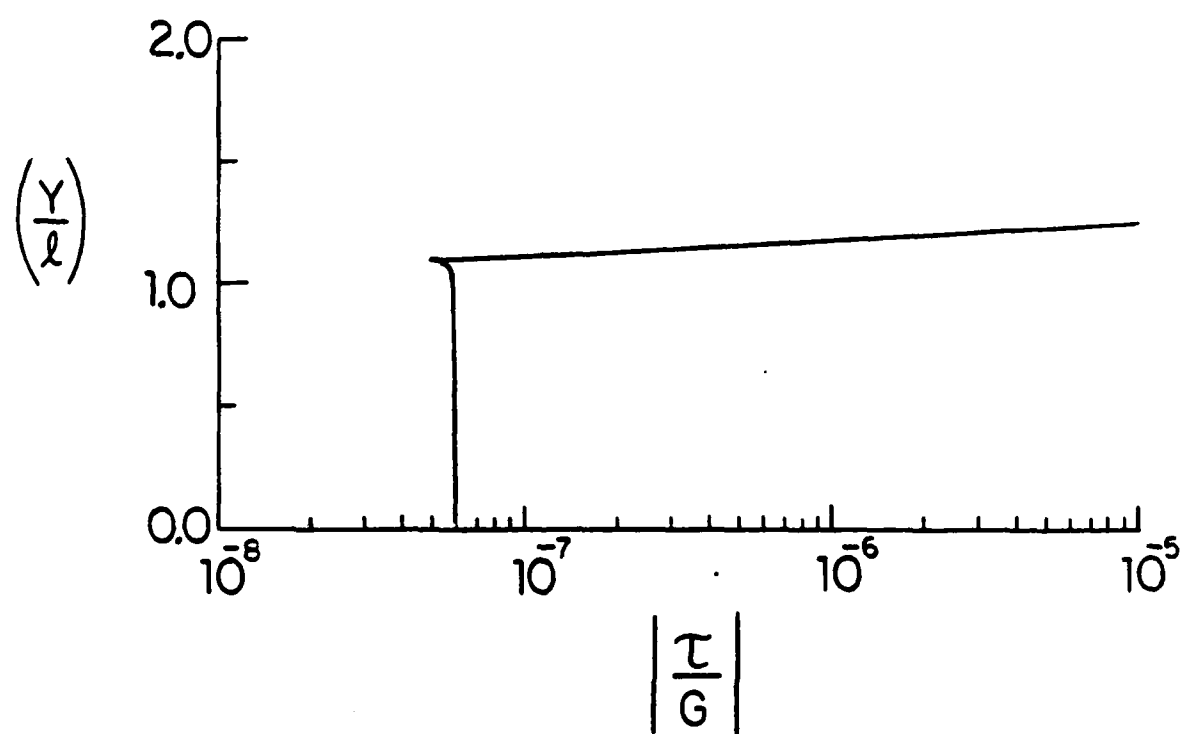


Fig. 22. Stress Distribution for a Stress-Driven Shear Disturbance
 $R = 10^{-5}$, $\Gamma = 50$, $h = 1.25$, $n = 32$.

APPENDIX I

Computer program used to evaluate displacement, stress and power distribution due to a unit displacement (or velocity) at $y=h$.

APPENDIX I

```

*****
*   D I S T U R E A N C E   I N   F L U I D   *
*****

S H E A R   W A V E S
V E L O C I T Y - D R I V E N
P A I N   P P O G R A M

DIMENSION Y(5),W(5),G(5),V1(3),V2(3),UU1(3),UU2(3)
COMPLEX COMPY1,COMPY2,RC,F,TAU,GAM,FIFIF
COMMON CR,C1,RB,RI,E
EXTERNAL DY
NSTOP=0

<<<<<<<<<<<<<<<<<<<<<<<<<<<<<<<<<<<<<<<<<<<< INPUT >>>>>>>>>>>>>>>>>>>>>>>>>>>>
<<<<<<<<<<<<<<<<<<<<<<<<<<<<<<<<<<<<<<<<<<<< DICTIONARY >>>>>>>>>>>>>>>>>>>>>>>>>>>>

NRUNS = NO. OF SETS OF RUNS.
NUM1 = NO. OF RUNS IN A GIVEN SET.
YNUM2 = POINTS BOUNDARY DETERMINING OUTPUT FORMAT.
NUM3 = DETERMINES WHICH POINTS ARE TO BE OUTPUTED
      WHEN THE ORDINATE Y IS LESS THAN OR EQUAL
      TO YNUM2.
NUM4 = DETERMINES WHICH POINTS ARE TO BE OUTPUTED
      WHEN THE ORDINATE Y IS GREATER THAN YNUM2.
ITER = 1 : ITERATE.
      2 : DO NOT ITERATE.
NITER = NO. OF ITERATIONS DESIRED.
PER = PERCENT BY WHICH THE INITIAL AND SUBSEQUENT
      VALUES OF DU (THE DERIVATIVE OF THE PARTICLE
      DISPLACEMENT) EVALUATED AT Y = 0 ARE TO
      INCREMENTED FOR THE CASE OF ITERATION.
Y(1) = VALUE OF THE ORDINATE ( Y ).
Y(2) = REAL PART OF THE PARTICLE DISPLACEMENT U.
Y(3) = IMAGINARY PART OF THE PARTICLE DISPLACEMENT U.
Y(4) = REAL PART OF THE DERIVATIVE OF THE PARTICLE
      DISPLACEMENT DU.
Y (5) = IMAGINARY PART OF THE DERIVATIVE OF THE
      PARTICLE DISPLACEMENT DU.
H = STEP SIZE FOR THE RUNGE-KUTTA:
    H1 = H IN THE INNER AND/OR OUTER REGIONS
    H2 = H IN THE MIDDLE OR OUTER REGIONS.
      (DEPENDING ON WHAT IS DESIRED)
CP = REAL PART OF GAMMA.
GI = IMAGINARY PART OF GAMMA = 0
PR = REAL PART OF R.
PI = IMAGINARY PART OF R = 0
E = N.
Z = VALUE OF THE ABSCISSA AT WHICH THE SOLUTIONS
      ARE SOUGHT.
LIM = NO. OF POINTS NEEDED FOR THE RUNGE-KUTTA.
      DETERMINES HOW FAR OUT WE GO IN THE Y-DIRECTION
      FOR A GIVEN STEP SIZE.
MBEG/NEND = DETERMINES THE REGION FOR WHICH H = H2.

<<<<<<<<<<<<<<<<<<<<<<<<<<<<<<<<<<<<<<<<<<<< * * * * >>>>>>>>>>>>>>>>>>>>>>>>>>>>
<<<<<<<<<<<<<<<<<<<<<<<<<<<<<<<<<<<<<<<<<<<< * * * * >>>>>>>>>>>>>>>>>>>>>>>>>>>>

READ(5,2)NRUNS
2  FORMAT(I2)
5  READ(5,10)NUM1,YNUM2,NUM3,NUM4,ITER,NITER,PER
  NSTOP=NSTOP+1
10 FORMAT(I2,F5.1,I5,I5,I1,I1,F7.5)
  WRITE(6,20)
20 FORMAT(1H1,EX,XY,EX,U(REAL),EX,U(IMAG),EX,U(MAG),EX,
1  TAU(REAL),EX,TAU(IMAG),EX,TAU(MAG),EX,WORK,EX,
1  H(REAL),EX,H(IMAG),EX,133('---'))

```



```

217: C      SLOPES ARE CALCULATED FOR EVERY OTHER ITERATION AFTER THE ZERO
218: C      GO TO (350,355,350,355,350,355,350,355,350,355),K
219: C      350  SP1=(UU1(2)-UU1(1))/(V1(2)-V1(1))
220: C      SP2=(UU2(2)-UU2(1))/(V1(2)-V1(1))
221: C      SN1=(UU1(3)-UU1(1))/(V2(3)-V2(1))
222: C      SN2=(UU2(3)-UU2(1))/(V2(3)-V2(1))
223: C      355  WRITE(6,360)SP1,SP2,SN1,SN2
224: C      360  FCPMAT(100(1-),/,1X,SLOPES: ,.4614,8,/,100(1-))
225: C      AAA=1.0-UU1(1)
226: C      BEB=-UU2(1)
227: C      DENOM=(SM1+SN2)-(SM2+SN1)
228: C      ALPHA=((AAA+SN2)-(BEB+SN1))/DENOM
229: C      BETA=((SM1+BEB)-(SM2+AAA))/DENOM
230: C      V1(1)=V1(1)+ALPHA
231: C      V2(1)=V2(1)+BETA
232: C      THE SAME SLOPES ARE USED FOR TWO CONSECUTIVE ITERATIONS.
233: C      GO TO (350,370,350,370,350,370,350,370,350,370),K
234: C      370  NJ=3
235: C      THESE VALUES ARE USED FOR THE TWO EXTRA RUNS NEEDED TO CALCULAT
236: C      NEW SLOPES.
237: C      V1(2)=V1(1)*(1.0+PER)
238: C      V2(2)=V2(1)
239: C      V1(3)=V1(1)
240: C      V2(3)=V2(1)*(1.0+PER)
241: C      GO TO 350
242: C      NJ=1
243: C      350  DUMMY=0.0
244: C
245: C      + + + + +
246: C      DO 470 J=1,NJ
247: C      JJ=J
248: C      IF((K.EC.NITER.AND.JJ.EQ.2)GO TO 500
249: C      ALL SYMBOLS FROM THIS POINT ON HAVE SAME MEANING AS THAT
250: C      SPECIFIED EARLIER.
251: C      Y(1)=YY1
252: C      Y(2)=YY2
253: C      Y(3)=YY3
254: C      Y(4)=V1(JJ)
255: C      Y(5)=V2(JJ)
256: C      Z=ZZ
257: C
258: C      X X X X I T E R A T I O N   R U N G E   -   K U T T A   X X X X X
259: C
260: C      THIS RUNGE-KUTTA LOOP IS THE SAME AS THAT USED PREVIOUSLY.
261: C      DO 450 N=1,LIM
262: C      IF(N.EG.1)WRITE(6,41)Y,H1,H2
263: C      IF(N.EG.1)WRITE(6,42)GP,GI,RR,RI,B,Z,LIM
264: C      H=H2
265: C      IF(N.LE.NEEG.OR.N.GT.NEND)H=H1
266: C      CALL PKTE(DY,Y,Z,H,W,Q,E)
267: C      COMPY1=CMPLY(Y(2),Y(3))
268: C      UMAG1=CABS(COMPY1)
269: C      COMPY2=CMPLY(Y(4),Y(5))
270: C      UMAG2=CABS(COMPY2)
271: C      IF(P.GT.EQ.C.AND.Y(1).GE.2.0)GO TO 395
272: C      ASSUME THAT AT Y=10 WE ARE OUTSIDE THE TRANSITION REGION
273: C      IF(Y(1).GE.10.0)GO TO 395
274: C      F=((1.-FC)*EXP(-(Y(1)*F)))+RC
275: C      GO TO 397
276: C      395  F=RC
277: C      397  TAU=COMPY2*F
278: C      TAU=CABS(TAU)
279: C      WORK=TAU*UMAG1
280: C      IF(Y(1).LE.YNUM2)GO TO 430
281: C      IF(MOD(N,NUM4).EQ.0.OR.N.EQ.1)WRITE(6,300)Y(1),Y(2),Y(3),UMAG1,
282: C      1TAU,TAU,WORK,F
283: C      GO TO 450
284: C      430  IF(MOD(N,NUM3).EQ.0.OR.N.EQ.1)WRITE(6,300)Y(1),Y(2),Y(3),UMAG1,
285: C      1TAU,TAU,WORK,F
286: C      450  CONTINUE

```

9012345678	C
8012345678	C
7012345678	C
6012345678	C
5012345678	C
4012345678	C
3012345678	C
2012345678	C
1012345678	C
0012345678	C

[illegible]

UNCLASSIFIED

SECURITY CLASSIFICATION OF THIS PAGE (When Data Entered)

REPORT DOCUMENTATION PAGE		READ INSTRUCTIONS BEFORE COMPLETING FORM
1. REPORT NUMBER SDSU/AE&EM/TR-83-01	2. GOVT ACCESSION NO. AD-A125 182	3. RECIPIENT'S CATALOG NUMBER
4. TITLE (and Subtitle) EFFECT OF AN INHOMOGENEOUS TRANSITION LAYER ON THE RESPONSE OF A COMPLIANT LAYER DUE TO A SHEAR FLUID DISTURBANCE		5. TYPE OF REPORT & PERIOD COVERED Final March 1982 - Nov. 1982
7. AUTHOR(s) Mauro Pierucci Paul Baxley		6. PERFORMING ORG. REPORT NUMBER AE&EM/TR-83-01
9. PERFORMING ORGANIZATION NAME AND ADDRESS Aerospace Engineering and Engineering Mechanics San Diego State University San Diego, CA 92182		8. CONTRACT OR GRANT NUMBER(s) N00014-81-K-0424
11. CONTROLLING OFFICE NAME AND ADDRESS Department of the Navy Office of Naval Research-Fluid Dynamics Arlington, VA 22217		10. PROGRAM ELEMENT, PROJECT, TASK AREA & WORK UNIT NUMBERS ONR 062-693
14. MONITORING AGENCY NAME & ADDRESS (if different from Controlling Office)		12. REPORT DATE Jan. 1983
		13. NUMBER OF PAGES 45 + 5 (appendices)
		15. SECURITY CLASS. (of this report) Unclassified
		15a. DECLASSIFICATION/DOWNGRADING SCHEDULE
16. DISTRIBUTION STATEMENT (of this Report) Approved for public release; distribution unlimited.		
17. DISTRIBUTION STATEMENT (of the abstract entered in Block 20, if different from Report)		
18. SUPPLEMENTARY NOTES		
19. KEY WORDS (Continue on reverse side if necessary and identify by block number) Drag reduction, inhomogeneous viscoelastic layer, fluid-structure interaction, shear waves, transverse waves.		
20. ABSTRACT (Continue on reverse side if necessary and identify by block number) The amount of interaction between a fluid and a compliant coating is studied for a one dimensional shear fluid disturbance. A thin inhomogeneous viscoelastic layer is located at the interface between the fluid and the coating. The fluid is assumed to have no mean flow field. The effect of different coating properties, thickness of compliant coating and of transition layer as well as the frequency of oscillations are analyzed.		

DD FORM 1 JAN 73 1473

EDITION OF 1 NOV 65 IS OBSOLETE
S/N 0102-LF-014-6601

UNCLASSIFIED

SECURITY CLASSIFICATION OF THIS PAGE (When Data Entered)

END.